Earthq Eng & Eng Vib (2020) 19: 377-395 **DOI**: https://doi.org/10.1007/s11803-020-0568-8

Dynamic response of a three-beam system with intermediate elastic connections under a moving load/mass-spring

Feng Yulin[1, 2†], Jiang Lizhong[1, 2‡] and Zhou Wangbao[1, 2§]

1. *School of Civil Engineering, Central South University, Changsha 410075, China*

2. *National Engineering Laboratory for High Speed Railway Construction, Central South University, Changsha 410075, China*

Abstract: The objective of this research is to study the dynamic response characteristics of a three-beam system with intermediate elastic connections under a moving load/mass-spring. In this study, the finite Sine-Fourier transform was performed for the dynamic partial differential equations of a simply supported three-beam system (SSTBS) under a moving load and a moving mass-spring, respectively. The dynamic partial differential equations were transformed into dynamic ordinary differential equations relative to the time coordinates, and the equations were solved and the displacement Fourier amplitude spectral expressions were obtained. Finally, based on finite Sine-Fourier inverse transform, the expressions for dynamic response of SSTBS under the moving load and moving mass-spring were obtained. The proposed method, along with ANSYS, was used to calculate the dynamic response of the SSTBS under a moving load/mass-spring at different speeds. The results obtained herein were consistent with the ANSYS numerical calculation results, verifying the accuracy of the proposed method. The influence of the load/mass-spring's moving speed on the dynamic deflections of SSTBS were analyzed. SSTBS has several critical speeds under a moving load/mass-spring. The vertical acceleration incurred by a change in the vertical speed of SSTBS due to the movement of mass-spring and the centrifugal acceleration produced by the movement of mass-spring on the vertical curve generated by SSTBS vibration could not be neglected.

Keywords: finite Sine-Fourier transform; three-beam system; moving load; mass-spring; critical speeds

1 Introduction

Beam-type structures are widely applied in mechanical, civil, and material engineering and many other fields; therefore, it is essential to accurately predict the vibration responses of these structures for engineering applications (Li *et al*., 2016; Li and Sun, 2016, 2017; Peng *et al*., 2017). Currently, studies on the vibration responses of beam-type structures under a moving load or a moving mass-spring have been conducted by researchers and engineers from various countries worldwide and encompass a broad field of emphasis (Bendine *et al*., 2016). There are numerous studies on the dynamic responses of single-beam systems under a moving load (Kumar *et al*., 2015; Liu *et al*., 2015; Wang and Ren, 2013). An important extension of the concept of a single-beam system is a double-beam system. Studies have also been reported on the vibration responses of double-beam, and a series of representative study methods have emerged as well (Rezaiee Pajand and Hozhabrossadati, 2014).

Shamalta and Metrikine (2003) investigated the steady-state dynamic response of an embedded railway track to a moving train theoretically, and developed a series of analytical formulas. Oniszczuk (2003) analyzed the undamped forced transverse vibrations of a double-beam system. The classical modal expansion method was used to determine the dynamic responses of beams due to arbitrarily distributed continuous loads. The action of moving forces was considered. Abu-hilal (2006) studied the dynamic response of a double-beam system traversed by a constant moving load. The dynamic deflections of both the beams were given in analytical closed forms. Using Fourier integral transforms, Zhang *et al*. (2008) studied two different loading conditions, a uniformly distributed harmonic load and a concentrated harmonic force applied at the midspan of the beam. Rusin *et al*. (2011) studied the dynamic behavior of a double-string system traversed by a constant or harmonically oscillating

Correspondence to: Zhou Wangbao, Department of Civil Engineering, Central South University, Changsha, China
Tel: +86-13677300601
E-mail: zhouwangbao@163.com
†PhD; ‡Professor; §Associate Professor

Supported by: The Fundamental Research Funds for the Central Universities of Central South University under Grant No. 2018zzts189, the National Natural Science Foundations of China under Grant Nos. 51408449 and 51778630, and the Innovation-driven Plan in Central South University under Grant No. 2015CX006
Received April 21, 2018; **Accepted** November 1, 2018

moving force, and the dynamic behavior of the double-string system traversed by a constant or harmonically oscillating moving force were given in closed solutions. In a recent study, Şimşek (2011) reported an analytical method to determine the forced vibration of an elastically connected double-carbon nanotube system carrying a moving nanoparticle based on the nonlocal elasticity theory. Then, Şimşek and Cansız (2012) studied the dynamic responses of an elastically connected double-functionally graded beam system carrying a moving harmonic load at a constant speed using the Euler-Bernoulli beam theory. Using the Adomian modified decomposition method, the researchers investigated the vibration problem of a cantilever double-beam system, stepped beams, and multi-stepped beams (Mao, 2011, 2015). Wu and Gao (2015) investigated the dynamic response of a simply supported viscously damped double-beam system under moving harmonic loads. Two coupled governing equations describing the vibration of the two beams were decoupled by a simple change of variables, achieving the analytical solutions for the dynamic deflections of both the beams.

Studies have also been carried out on the dynamic responses of double-beam systems under a moving mass-spring. The dynamic response of double-beam under a moving mass-spring was investigated by different methods. A suitable single-step scheme was provided for the numerical integration of the equations of motion, and dimensional analysis was applied in order to define the dimensionless combinations of the design parameters that dictate the responses of the beam and moving mass-spring (Muscolino and Palmeri, 2007). Using Laplace and Fourier transformations, Zheng (2000) developed an analytical method which can analyze a rail modeled as an infinite beam on a viscoelastic foundation, subjected to a moving vehicle modeled as a mass-spring-damper system. Using the method of modal superposition, Yang and Lin (2005) discussed the influence of the driving frequency of the moving structure and the natural frequencies of the beam upon the dynamic response. Based on the nonlocal elasticity theory, Şimşek (2010) developed an analytical method for the forced vibration of an elastically connected double-carbon nanotube system carrying a moving mass-spring. And the problem was also solved numerically by using the Galerkin method and the time integration method of Newmark to verify the reliability of the analytical method (Şimşek, 2015). The coupled equations governing the vibration of double-beam system under a moving mass-spring have been decoupled by a simple change. Then, a state-space equation governing the vibration of the two beams and a moving mass-spring has been established by introducing some state variables, and solved by a single-step scheme (Wu and Gao, 2016). Dimitrovová (2017) developed a new semi-analytical solution for the moving mass problem on infinite beams and it was derived in the form of an analytical closed form formula for a loading point displacement.

However, due to the complexity of the three-beam, previous studies on the vibration problems of three-beam under a moving load/mass-spring were mostly aimed at its vibration characteristics. As an early fundamental work, Abu-Hilal (2007) analyzed the free vibrational behavior of an undamped three-beam system. The natural frequencies and mode shapes of the system have been determined and discussed in detail. Also, the effects of layer stiffnesses and the masses per unit length of the beams on the natural frequencies and mode shapes of the system have been explored. Li *et al*. (2008) developed a dynamic stiffness method for a three-beam system. The dynamic stiffness matrix has been formulated from the analytical closed-form solutions of the differential equations of motion of the three-beam element in free transverse vibration. An exact dynamic stiffness method is developed for predicting the free vibration characteristics of a three-beam system, which is composed of three non-identical uniform beams of equal length connected by innumerable coupling springs and dashpots (Li and Hua, 2008). To sum up, the methods for studying the dynamic responses of SSTBS under a moving load/mass-spring mostly suffer from complex deductions, numerous restrictions, and low calculation efficiency. The dynamic responses of SSTBS have been rarely studied.

In this study, the finite Sine-Fourier transform was performed for the dynamic partial differential equations of SSTBS under a moving load and a moving mass-spring, respectively, the dynamic partial differential equations were transformed into dynamic ordinary differential equations relative to the time coordinates, and furthermore the equations had been solved and obtained the displacement Fourier amplitude spectral expressions. Finally, based on finite Sine-Fourier inverse transform, the expressions for dynamic response of SSTBS under the moving load and moving mass-spring were obtained, respectively. The proposed method along with ANSYS were used to calculate the dynamic response of SSTBS under a moving load/mass-spring at different speeds, the results obtained in this study were consistent with the ANSYS numerical calculation results, verifying the accuracy of the proposed method. Compared with the numerical simulation analysis, the analytic method can incarnate the key influence factors and their influence laws affecting the dynamic response of structures more intuitively, provide a theoretical basis for deriving a practical formula for engineering calculation and make up the deficiency of numerical simulation analysis, for example, numerical simulations cannot account for the effects of the latter two terms. The proposed method in this paper can be apply in mechanical, civil, traffic and material engineering and many other fields. For example, the dynamic behavior of the bridge-track system of railway (maglev) under the train load can be studied by using the proposed method.

2 Mathematical model and governing equations

2.1 Dynamic response of SSTBS under a moving load

2.1.1 Coupled partial differential equations

In this study, the physical model of a three-beam system is composed of the first layer beam (layer-I), second layer beam (layer-II) and third layer beam (layer-III) joined by intermediate elastic connections, and the physical model of a SSTBS is shown in Fig. 1 (Şimşek, 2010, 2015). All the beams are homogeneous, prismatic, and have the same length L, but can have different mass or flexural rigidity, which makes the model more realistic.

The vertical vibration of the three-beam system shown in Fig. 1 is governed by the following three coupled partial differential equations (Ni and Zhang, 2018; Sun *et al*., 2015).

$$E_1 I_1 \frac{\partial^4 y_1}{\partial x^4} + m_1 \frac{\partial^2 y_1}{\partial t^2} + c_1 \frac{\partial (y_1 - y_2)}{\partial t} + k_1 (y_1 - y_2) = P_0 \delta (x - vt) \tag{1}$$

$$E_2 I_2 \frac{\partial^4 y_2}{\partial x^4} + m_2 \frac{\partial^2 y_2}{\partial t^2} - c_1 \frac{\partial (y_1 - y_2)}{\partial t} + c_2 \frac{\partial (y_2 - y_3)}{\partial t} - k_1 (y_1 - y_2) + k_2 (y_2 - y_3) = 0 \tag{2}$$

$$E_3 I_3 \frac{\partial^4 y_3}{\partial x^4} + m_3 \frac{\partial^2 y_3}{\partial t^2} + c_2 \frac{\partial (y_3 - y_2)}{\partial t} + k_2 (y_3 - y_2) = 0 \tag{3}$$

where $y_1(x,t), y_2(x,t), y_3(x,t)$; E_1, E_2, E_3; I_1, I_2, I_3; m_1, m_2, m_3 denote the vertical deflections, elastic modulus, horizontal moments of inertia, and per-unit-length beam masses of layer-I, layer-II, and layer-III, respectively; k_1, k_2, c_1, c_2 denote the spring stiffness and damping value of the Winkler layer between layer-I and layer-II beams and that of the Winkler layer between layer-II and layer-III, respectively (Wu and Gao, 2016; Zhai and Cai, 2011); δ denotes the Dirac function; v denotes the load moving speed; and $P(t) = P_0 \delta (x - vt)$, P_0 denotes the moving load intensity.

2.1.2 Finite Sine-Fourier transform

To solve the above-mentioned partial differential equations of vibration, a finite Sine-Fourier transform for space coordinate x is used, and for $0 \le x \le L$, it is defined as follows:

$$F[y_1(x,t)] = U_{1,k}(t) = \int_0^L y_1(x,t) \sin(\xi_k x) \mathrm{d}x \tag{4}$$

$$F[y_2(x,t)] = U_{2,k}(t) = \int_0^L y_2(x,t) \sin(\xi_k x) \mathrm{d}x \tag{5}$$

$$F[y_3(x,t)] = U_{3,k}(t) = \int_0^L y_3(x,t) \sin(\xi_k x) \mathrm{d}x \tag{6}$$

$$F^{-1}[U_{1,k}(t)] = y_1(x,t) = \frac{2}{L} \sum_{k=1}^{\infty} U_{1,k}(t) \sin(\xi_k x) \tag{7}$$

$$F^{-1}[U_{2,k}(t)] = y_2(x,t) = \frac{2}{L} \sum_{k=1}^{\infty} U_{2,k}(t) \sin(\xi_k x) \tag{8}$$

$$F^{-1}[U_{3,k}(t)] = y_3(x,t) = \frac{2}{L} \sum_{k=1}^{\infty} U_{3,k}(t) \sin(\xi_k x) \tag{9}$$

$$\xi_k = \frac{k\pi}{L}, \quad k = 1,2,3,... \tag{10}$$

where, although k is between $1 \sim \infty$, taking $N \ge 30$ items can generally meet the accuracy requirement of engineering calculations (Ba *et al*., 2018). Next, Eqs. (7)-(9) can be simplified as follows

$$F^{-1}[U_{1,k}(t)] = y_1(x,t) = \frac{2}{L} \sum_{k=1}^{N} U_{1,k}(t) \sin(\xi_k x) \tag{11}$$

$$F^{-1}[U_{2,k}(t)] = y_2(x,t) = \frac{2}{L} \sum_{k=1}^{N} U_{2,k}(t) \sin(\xi_k x) \tag{12}$$

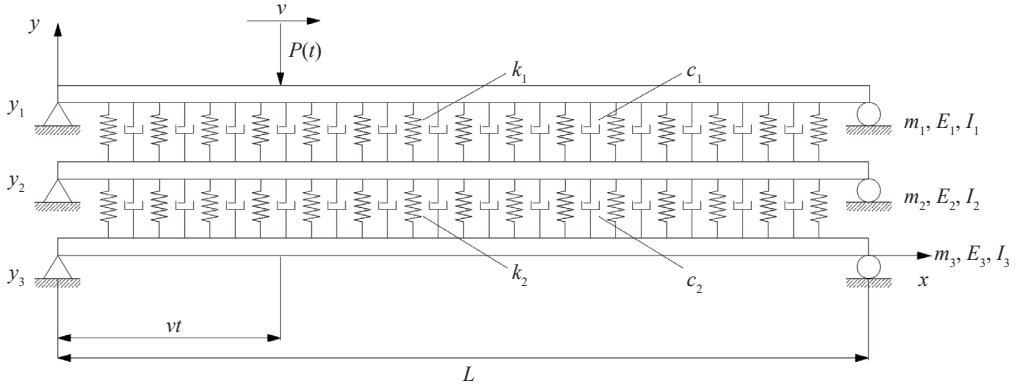

Fig. 1 Physical model of SSTBS under a moving load

$$F^{-1}\left[U_{3,k}(t)\right]=y_3(x,t)=\frac{2}{L}\sum_{k=1}^{N}U_{3,k}(t)\sin(\xi_k x) \quad (13)$$

Under minor deformation conditions, the boundary condition of a simply supported beam can be written as follows (Luo *et al*., 2017):

$$y_1(x,t)\big|_{x=0,L}=0,\quad EIy_1''(x,t)\big|_{x=0,L}=0 \quad (14)$$

$$y_2(x,t)\big|_{x=0,L}=0,\quad EIy_2''(x,t)\big|_{x=0,L}=0 \quad (15)$$

$$y_3(x,t)\big|_{x=0,L}=0,\quad EIy_3''(x,t)\big|_{x=0,L}=0 \quad (16)$$

According to the boundary condition, the finite Sine-Fourier transform of the fourth-order derivative of the displacement function relative to coordinate x can be obtained as follows:

$$F\left\{\frac{\mathrm{d}^4y_1(x,t)}{\mathrm{d}x^4}\right\}=\xi_k^4U_{1,k}(t) \quad (17)$$

$$F\left\{\frac{\mathrm{d}^4y_2(x,t)}{\mathrm{d}x^4}\right\}=\xi_k^4U_{2,k}(t) \quad (18)$$

$$F\left\{\frac{\mathrm{d}^4y_3(x,t)}{\mathrm{d}x^4}\right\}=\xi_k^4U_{3,k}(t) \quad (19)$$

By performing finite Sine-Fourier transform for both sides of Eqs. (1)-(3) relative to coordinate x,

$$E_1I_1\xi_k^4U_{1,k}(t)+m_1\frac{\partial^2}{\partial t^2}U_{1,k}(t)+c_1\frac{\partial}{\partial t}U_{1,k}(t)-c_1\frac{\partial}{\partial t}U_{2,k}(t)+k_1U_{1,k}(t)-k_1U_{2,k}(t)=P_0\sin\xi_k vt \quad (20)$$

$$E_2I_2\xi_k^4U_{2,k}(t)+m_2\frac{\partial^2}{\partial t^2}U_{2,k}(t)-c_1\frac{\partial}{\partial t}\left(U_{1,k}(t)-U_{2,k}(t)\right)+c_2\frac{\partial}{\partial t}\left(U_{2,k}(t)-U_{3,k}(t)\right)-k_1\left(U_{1,k}(t)-U_{2,k}(t)\right)+k_2\left(U_{2,k}(t)-U_{3,k}(t)\right)=0 \quad (21)$$

$$E_3I_3\xi_k^4U_{3,k}(t)+m_3\frac{\partial^2}{\partial t^2}U_{3,k}(t)+c_2\frac{\partial}{\partial t}\left(U_{3,k}(t)-U_{2,k}(t)\right)+k_2\left(U_{3,k}(t)-U_{2,k}(t)\right)=0 \quad (22)$$

Equations (20)-(22) can be further expressed as follows (Zhang *et al*., 2016):

$$\boldsymbol{M}_k\frac{\mathrm{d}^2}{\mathrm{d}t^2}\boldsymbol{U}_k+\boldsymbol{C}_k\frac{\mathrm{d}}{\mathrm{d}t}\boldsymbol{U}_k+\boldsymbol{K}_k\boldsymbol{U}_k=\boldsymbol{P}_k(t) \quad (23)$$

$$\boldsymbol{K}_k=\begin{bmatrix}E_1I_1\xi_k^4+k_1 & -k_1 & 0\\ -k_1 & E_2I_2\xi_k^4+k_1+k_2 & -k_2\\ 0 & -k_2 & E_3I_3\xi_k^4+k_2\end{bmatrix} \quad (24)$$

$$\boldsymbol{C}_k=\begin{bmatrix}c_1 & -c_1 & 0\\ -c_1 & c_1+c_2 & -c_2\\ 0 & -c_2 & c_2\end{bmatrix} \quad (25)$$

$$\boldsymbol{M}_k=\begin{bmatrix}m_1 & & \\ & m_2 & \\ & & m_3\end{bmatrix} \quad (26)$$

$$\boldsymbol{U}_k=\left(U_{1,k},U_{2,k},U_{3,k}\right)^{\mathrm{T}},\ \boldsymbol{P}_k=\left(P_0\sin\xi_k vt,0,0\right)^{\mathrm{T}} \quad (27)$$

By providing the coordinates canonical transformation for Fourier amplitude spectrum $\boldsymbol{U}_k$,

$$\boldsymbol{U}_k=\boldsymbol{\phi}_k\boldsymbol{q}_k \quad (28)$$

$$\boldsymbol{q}_k=\left(q_{1,k},q_{2,k},q_{3,k}\right)^{\mathrm{T}} \quad (29)$$

$$\boldsymbol{\phi}_k=\left[\{\boldsymbol{\phi}_k\}_1,\{\boldsymbol{\phi}_k\}_2,\{\boldsymbol{\phi}_k\}_3\right] \quad (30)$$

where, $\boldsymbol{\phi}_k$ denotes the generalized eigenvector matrix of matrix $\boldsymbol{K}_k$ relative to matrix $\boldsymbol{M}_k$; and $\boldsymbol{q}_k$ denotes the generalized coordinate vector.

By substituting Eq. (28) into Eq. (23),

$$\boldsymbol{M}_k\boldsymbol{\phi}_k\frac{\mathrm{d}^2}{\mathrm{d}t^2}\boldsymbol{q}_k+\boldsymbol{C}_k\boldsymbol{\phi}_k\frac{\mathrm{d}}{\mathrm{d}t}\boldsymbol{q}_k+\boldsymbol{K}_k\boldsymbol{\phi}_k\boldsymbol{q}_k=\boldsymbol{P}_k \quad (31)$$

By pre-multiplying both sides of Eq. (31) with $\boldsymbol{\phi}_k^{\mathrm{T}}$,

$$\boldsymbol{\phi}_k^{\mathrm{T}}\boldsymbol{M}_k\boldsymbol{\phi}_k\frac{\mathrm{d}^2}{\mathrm{d}t^2}\boldsymbol{q}_k+\boldsymbol{\phi}_k^{\mathrm{T}}\boldsymbol{C}_k\boldsymbol{\phi}_k\frac{\mathrm{d}}{\mathrm{d}t}\boldsymbol{q}_k+\boldsymbol{\phi}_k^{\mathrm{T}}\boldsymbol{K}_k\boldsymbol{\phi}_k\boldsymbol{q}_k=\boldsymbol{\phi}_k^{\mathrm{T}}\boldsymbol{P}_k \quad (32)$$

Using classical damping, $\boldsymbol{C}_k$, $\boldsymbol{K}_k$ and $\boldsymbol{M}_k$ are all symmetric positive definite matrices; considering the weighted orthogonality of the generalized eigenvector relative to $\boldsymbol{C}_k$, $\boldsymbol{K}_k$ and $\boldsymbol{M}_k$, Eq. (32) can be simplified as follows (Sun *et al*., 2015):

$$\frac{\mathrm{d}^2}{\mathrm{d}t^2}q_{n,k}(t)+2\zeta_{n,k}\omega_{n,k}\frac{\mathrm{d}}{\mathrm{d}t}q_{n,k}(t)+\omega_{n,k}^2 q_{n,k}(t)=\frac{1}{M_{n,k}}P_{n,k}(t)\quad n=1,2,3 \tag{33}$$

$$q_{n,k}(t)=q_{n,k}^{\mathrm{s}}(t)+q_{n,k}^{0}(t) \tag{34}$$

$$M_{n,k}=\boldsymbol{\phi}_{kn}^{\mathrm{T}}\boldsymbol{M}_k\boldsymbol{\phi}_{kn} \tag{35}$$

$$K_{n,k}=\boldsymbol{\phi}_{kn}^{\mathrm{T}}\boldsymbol{M}_k\boldsymbol{\phi}_{kn} \tag{36}$$

$$C_{n,k}=\boldsymbol{\phi}_{kn}^{\mathrm{T}}\boldsymbol{M}_k\boldsymbol{\phi}_{kn} \tag{37}$$

$$\omega_{n,k}^2=K_{n,k}/M_{n,k} \tag{38}$$

$$\zeta_{n,k}=C_{n,k}/2\omega_{n,k}M_{n,k} \tag{39}$$

$$P_{n,k}=\boldsymbol{\phi}_{kn}^{\mathrm{T}}\boldsymbol{P}_k \tag{40}$$

where, $q_{n,k}^{\mathrm{s}}(t)$ denotes the solution of Eq. (33), and $q_{n,k}^{0}(t)$ denotes the homogeneous solution of Eq. (33).

Through Duhamel integral (Sun *et al*., 2016) the particular solution of Eq. (33) with zero initial conditions can be obtained as follows:

$$q_{n,k}^{\mathrm{s}}(t)=\frac{1}{M_{n,k}\omega_{Dn,k}}\cdot\int_0^t P_{n,k}(\tau)\mathrm{e}^{-\zeta_{n,k}\omega_{n,k}(t-\tau)}\sin\left[\omega_{Dn,k}(t-\tau)\right]\mathrm{d}\tau \tag{41}$$

$$\omega_{Dn,k}=\omega_{n,k}\sqrt{1-\zeta_{n,k}^2} \tag{42}$$

$$q_{n,k}^{\mathrm{s}}(t)=\frac{\boldsymbol{\phi}_{kn}^{\mathrm{T}}}{2M_{n,k}\omega_{Dn,k}}\cdot\left\{\begin{array}{c}\dfrac{P_0\left(\cos\xi_k vt-\mathrm{e}^{-\zeta_{n,k}\omega_{n,k}t}\cos\left(-\omega_{Dn,k}t\right)\right)\left(\zeta_{n,k}\omega_{n,k}\right)+P_0\left(\xi_k v+\omega_{Dn,k}\right)\left(\sin\xi_k vt-\mathrm{e}^{-\zeta_{n,k}\omega_{n,k}t}\sin\left(-\omega_{Dn,k}t\right)\right)}{\left(\zeta_{n,k}\omega_{n,k}\right)^2+\left(\xi_k v+\omega_{Dn,k}\right)^2}\\ -\dfrac{P_0\left(\cos\xi_k vt-\mathrm{e}^{-\zeta_{n,k}\omega_{n,k}t}\cos\omega_{Dn,k}t\right)\left(\zeta_{n,k}\omega_{n,k}\right)+P_0\left(\xi_k v-\omega_{Dn,k}\right)\left(\sin\xi_k vt-\mathrm{e}^{-\zeta_{n,k}\omega_{n,k}t}\sin\omega_{Dn,k}t\right)}{\left(\xi_k v-\omega_{Dn,k}\right)^2+\left(\zeta_{n,k}\omega_{n,k}\right)^2}\\ 0\\ 0\end{array}\right\} \tag{43}$$

2.1.3 Solving the equation

Using Eqs. (4)-(6),

$$U_{n,k}(0)=\int_0^L y_n(x,0)\sin\left(\xi_k x\right)\mathrm{d}x \tag{44}$$

$$\frac{\mathrm{d}}{\mathrm{d}t}U_{n,k}(0)=\int_0^L\frac{\mathrm{d}}{\mathrm{d}t}y_n(x,0)\sin\left(\xi_k x\right)\mathrm{d}x \tag{45}$$

Using Eq. (28),

$$\boldsymbol{U}_k(0)=\sum_{n=1}^{3}\boldsymbol{\phi}_{kn}q_{n,k}^{0}(0) \tag{46}$$

$$\frac{\mathrm{d}}{\mathrm{d}t}\boldsymbol{U}_k(0)=\sum_{n=1}^{3}\boldsymbol{\phi}_{kn}\frac{\mathrm{d}}{\mathrm{d}t}q_{n,k}^{0}(0) \tag{47}$$

By multiplying the left side of Eqs. (46)-(47) with $\boldsymbol{\phi}_{kn}^{\mathrm{T}}\boldsymbol{M}_k$ and using weighted orthogonality,

$$q_{n,k}^{0}(0)=\frac{\boldsymbol{\phi}_{kn}^{\mathrm{T}}\boldsymbol{M}_k\boldsymbol{U}_k(0)}{M_{n,k}} \tag{48}$$

$$\frac{\mathrm{d}}{\mathrm{d}t}q_{n,k}^{0}(0)=\frac{\boldsymbol{\phi}_{kn}^{\mathrm{T}}\boldsymbol{M}_k\dfrac{\mathrm{d}}{\mathrm{d}t}\boldsymbol{U}_k(0)}{M_{n,k}} \tag{49}$$

Using Eqs. (48)-(49), the homogeneous solution of Eq. (33) can be obtained by considering the initial conditions (Ni and Zhang, 2018; Zhang *et al*., 2014):

$$q_{n,k}^{0}(t)=\mathrm{e}^{-\zeta_{n,k}\omega_{n,k}t}\cdot\left[q_{n,k}^{0}(0)\cos\left(\omega_{Dn,k}t\right)+\frac{\dfrac{\mathrm{d}}{\mathrm{d}t}q_{n,k}^{0}(0)+\zeta_{n,k}\omega_{n,k}q_{n,k}^{0}(0)}{\omega_{Dn,k}}\sin\left(\omega_{Dn,k}t\right)\right] \tag{50}$$

By substituting Eqs. (50) and (43) into (34),

$$q_{n,k}(t)=\frac{\boldsymbol{\phi}_{kn}^{\mathrm{T}}}{2M_{n,k}\omega_{Dn,k}}\cdot\left\{\begin{array}{c}\dfrac{P_0\left(\cos\xi_k vt-\mathrm{e}^{-\zeta_{n,k}\omega_{n,k}t}\cos\left(-\omega_{Dn,k}t\right)\right)\left(\zeta_{n,k}\omega_{n,k}\right)+P_0\left(\xi_k v+\omega_{Dn,k}\right)\left(\sin\xi_k vt-\mathrm{e}^{-\zeta_{n,k}\omega_{n,k}t}\sin\left(-\omega_{Dn,k}t\right)\right)}{\left(\zeta_{n,k}\omega_{n,k}\right)^2+\left(\xi_k v+\omega_{Dn,k}\right)^2}\\ -\dfrac{P_0\left(\cos\xi_k vt-\mathrm{e}^{-\zeta_{n,k}\omega_{n,k}t}\cos\omega_{Dn,k}t\right)\left(\zeta_{n,k}\omega_{n,k}\right)+P_0\left(\xi_k v-\omega_{Dn,k}\right)\left(\sin\xi_k vt-\mathrm{e}^{-\zeta_{n,k}\omega_{n,k}t}\sin\omega_{Dn,k}t\right)}{\left(\xi_k v-\omega_{Dn,k}\right)^2+\left(\zeta_{n,k}\omega_{n,k}\right)^2}\\ 0\\ 0\end{array}\right\}+\mathrm{e}^{-\zeta_{n,k}\omega_{n,k}t}\left[q_{n,k}^{0}(0)\cos\left(\omega_{Dn,k}t\right)+\frac{\dfrac{\mathrm{d}}{\mathrm{d}t}q_{n,k}^{0}(0)+\zeta_{n,k}\omega_{n,k}q_{n,k}^{0}(0)}{\omega_{Dn,k}}\sin\left(\omega_{Dn,k}t\right)\right] \tag{51}$$

When SSTBS has zero initial conditions,

$$U_{n,k}(0)=0,\ \frac{\mathrm{d}}{\mathrm{d}t}U_{n,k}(0)=0 \tag{52}$$

$$q_{n,k}^{0}(0)=0,\ \frac{\mathrm{d}}{\mathrm{d}t}q_{n,k}^{0}(0)=0 \tag{53}$$

Equation (51) can be simplified as follows:

$$q_{n,k}^{s}(t)=\frac{\boldsymbol{\phi}_n^{\mathrm{T}}}{2M_{n,k}\omega_{Dn,k}}\cdot \begin{Bmatrix} \dfrac{P_0\left(\cos\xi_k vt-\mathrm{e}^{-\zeta_{n,k}\omega_{n,k}t}\cos\left(-\omega_{Dn,k}t\right)\right)\left(\zeta_{n,k}\omega_{n,k}\right)+P_0\left(\xi_k v+\omega_{Dn,k}\right)\left(\sin\xi_k vt-\mathrm{e}^{-\zeta_{n,k}\omega_{n,k}t}\sin\left(-\omega_{Dn,k}t\right)\right)}{\left(\zeta_{n,k}\omega_{n,k}\right)^2+\left(\xi_k v+\omega_{Dn,k}\right)^2} \\ -\dfrac{P_0\left(\cos\xi_k vt-\mathrm{e}^{-\zeta_{n,k}\omega_{n,k}t}\cos\omega_{Dn,k}t\right)\left(\zeta_{n,k}\omega_{n,k}\right)+P_0\left(\xi_k v-\omega_{D_{n,k}}\right)\left(\sin\xi_k vt-\mathrm{e}^{-\zeta_{n,k}\omega_{n,k}t}\sin\omega_{D_{n,k}}t\right)}{\left(\xi_k v-\omega_{D_{n,k}}\right)^2+\left(\zeta_{n,k}\omega_{n,k}\right)^2} \\ 0 \\ 0 \end{Bmatrix} \tag{54}$$

By simultaneously solvig Eqs. (9), (28), (29), and (51),

$$\boldsymbol{y}=\frac{2}{L}\sum_{k=1}^{N}\boldsymbol{\phi}_k\boldsymbol{q}_k\sin\xi_k x \tag{55}$$

where $\boldsymbol{y}=\left(y_1,y_2,y_3\right)^{\mathrm{T}}$.

2.2 Dynamic response of SSTBS under a moving mass-spring

2.2.1 Coupled partial differential equations

The physical model of SSTBS under a moving mass-spring is shown in Fig. 2. All of the beams are homogeneous, prismatic, and the same length L, but they can have different mass or flexural rigidity, which me actual engineering projects.

According to the d′Alembert principle, the dynamic equilibrium equation of a mass-spring can be expressed as (Sun *et al*., 2015)

$$M_2\frac{\partial^2 Z(t)}{\partial t^2}+c_0\frac{\partial\left[Z(t)-y_1(x,t)\right]}{\partial t}+k_0\left[Z(t)-y_1(x,t)\right]=0 \tag{56}$$

where M_2 represents the sprung mass; $Z(t)$ represents the dynamic displacement of the sprung mass; c_0 represents the damping coefficient of the mass-spring system (Li, 2018); and k_0 represents the spring coefficient of the mass-spring system.

According to the d′Alembert principle, thedynamic equilibrium equations system of a SSTBS and mass-spring can be expressed as (Ni and Zhang, 2018; Sun *et al*., 2015; Yan and Ren, 2013):

$$E_1I_1\frac{\partial^4 y_1(x,t)}{\partial x^4}+m_1\frac{\partial^2 y_1(x,t)}{\partial t^2}+ c_1\frac{\partial\left[y_1(x,t)-y_2(x,t)\right]}{\partial t}+k_1\left[y_1(x,t)-y_2(x,t)\right]=P_0(t) \tag{57}$$

$$E_2I_2\frac{\partial^4 y_2(x,t)}{\partial x^4}+m_2\frac{\partial^2 y_2(x,t)}{\partial t^2}-c_1\frac{\partial\left[y_1(x,t)-y_2(x,t)\right]}{\partial t}+ c_2\frac{\partial\left[y_2(x,t)-y_3(x,t)\right]}{\partial t}-k_1\left[y_1(x,t)-y_2(x,t)\right]+ k_2\left[y_2(x,t)-y_3(x,t)\right]=0 \tag{58}$$

$$E_3I_3\frac{\partial^4 y_3(x,t)}{\partial x^4}+m_3\frac{\partial^2 y_3(x,t)}{\partial t^2}+ c_2\frac{\partial\left[y_3(x,t)-y_2(x,t)\right]}{\partial t}+k_2\left[y_3(x,t)-y_2(x,t)\right]=0 \tag{59}$$

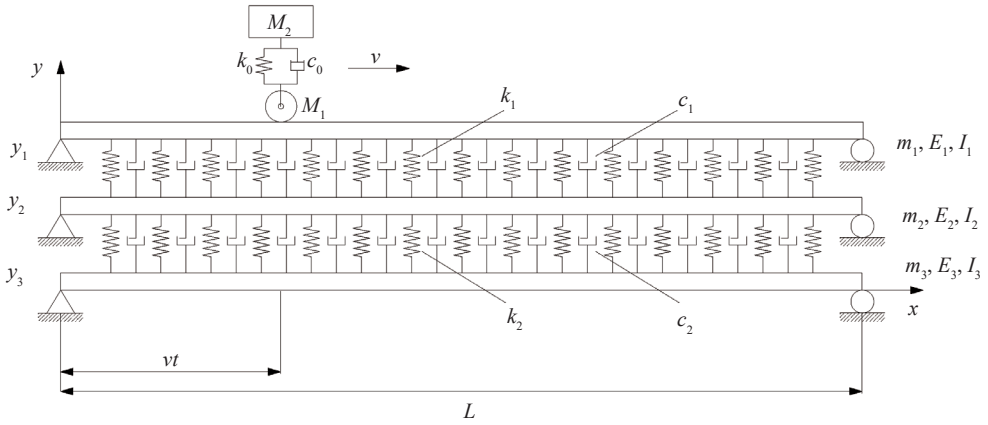

Fig. 2 Physical model of SSTBS under a moving mass-spring

The external loads along the direction of the displacement degree of freedom can be expressed as (Wu , 2016):

$$P_0(t)=\delta(x-vt)\left[(M_1+M_2)\mathrm{g}-M_1\left(\frac{\partial^2 y_1}{\partial t^2}+2v\frac{\partial^2 y_1}{\partial x\partial t}+v^2\frac{\partial^2 y_1}{\partial x^2}\right)+c_0\left(\frac{\partial}{\partial t}Z(t)-\frac{\partial y_1}{\partial t}-v\frac{\partial y_1}{\partial x}\right)+k_0\left(Z(t)-y_1\right)\right] \tag{60}$$

where M_1 represents the unsprung mass; v represents the moving speed of the mass-spring; $P_0(t)$ represents the external force; g represents the acceleration of gravity.

2.2.2 Finite Sine-Fourier transform

To solve the above vibration artial differential equations system, the first step is to provide finite Sine-Fourier transform on the space coordinate x, and for $0\le x\le L$, finite Sine-Fourier transform can be defined as Eqs. (4)-(9). Under minor deformation conditions, the boundary condition of the SSTBS can be written as Eqs. (14)-(16). Based on the boundary conditions, the finite Sine-Fourier transform of the fourth derivative of the displacement function is the same as Eqs. (17)-(19). By performing finite Sine-Fourier transform for both sides of Eqs. (1)-(60) relative to coordinate x, to both sides of Eqs. (56)-(60), the dynamic ordinary differential equations of the SSTBS with respect to time coordinates can be expressed as

$$\begin{aligned}&E_1I_1\xi_k^4U_{1,k}(t)+m_1\frac{\partial^2}{\partial t^2}U_{1,k}(t)+k_1U_{1,k}(t)-k_1U_{2,k}(t)+c_1\frac{\partial}{\partial t}U_{1,k}(t)-\\&c_1\frac{\partial}{\partial t}U_{2,k}(t)+M_1\sin\xi_kvt\frac{2}{L}\sum_{i=1}^{N}\frac{\partial^2}{\partial t^2}U_{1,i}(t)\sin\xi_ivt+\\&M_1\sin\xi_kvt2\frac{2}{L}v\sum_{i=1}^{N}\xi_i\frac{\partial}{\partial t}U_{1,i}(t)\cos\xi_ivt-\\&M_1\sin\xi_kvt\frac{2}{L}v^2\sum_{i=1}^{N}(\xi_i)^2U_{1,i}(t)\sin\xi_ivt-k_0\left(Z(t)\right)\sin\xi_kvt+\\&k_0\frac{2}{L}\sum_{i=1}^{N}U_{1,i}(t)\sin\xi_ivt\sin\xi_kvt-c_0\left(\frac{\partial}{\partial t}Z(t)\right)\sin\xi_kvt+\\&c_0\frac{2}{L}\sin\xi_kvt\sum_{i=1}^{N}\frac{\partial}{\partial t}U_{1,i}(t)\sin\xi_ivt+\\&c_0v\frac{2}{L}\sin\xi_kvt\sum_{i=1}^{N}\xi_iU_{1,i}(t)\cos\xi_ivt=(M_1+M_2)\mathrm{g}\sin\xi_kvt\end{aligned} \tag{61}$$

$$\begin{aligned}&E_2I_2\xi_k^4U_{2,\mathrm{k}}(t)+m_2\frac{\partial^2}{\partial t^2}U_{2,\mathrm{k}}(t)-c_1\frac{\partial}{\partial t}\left(U_{1,\mathrm{k}}(t)-U_{2,\mathrm{k}}(t)\right)+\\&c_2\frac{\partial}{\partial t}\left(U_{2,\mathrm{k}}(t)-U_{3,\mathrm{k}}(t)\right)-k_1\left(U_{1,\mathrm{k}}(t)-U_{2,\mathrm{k}}(t)\right)+\\&k_2\left(U_{2,\mathrm{k}}(t)-U_{3,\mathrm{k}}(t)\right)=0\end{aligned} \tag{62}$$

$$\begin{aligned}&E_3I_3\xi_k^4U_{3,\mathrm{k}}(t)+m_3\frac{\partial^2}{\partial t^2}U_{3,\mathrm{k}}(t)+\\&c_2\frac{\partial}{\partial t}\left(U_{3,\mathrm{k}}(t)-U_{2,\mathrm{k}}(t)\right)+k_2\left(U_{3,\mathrm{k}}(t)-U_{2,\mathrm{k}}(t)\right)=0\end{aligned} \tag{63}$$

$$\begin{aligned}&\frac{L}{2}M_2\frac{\partial^2}{\partial t^2}Z(t)+\frac{L}{2}k_0Z(t)-k_0\sum_{i=1}^{N}U_{1,\mathrm{i}}(t)\sin\xi_ivt+\\&c_0\frac{\partial}{\partial t}Z(t)-c_0\sum_{i=1}^{N}\frac{\partial}{\partial t}U_{1,\mathrm{i}}(t)\sin\xi_ivt-c_0v\sum_{i=1}^{N}\xi_iU_{1,\mathrm{i}}(t)\cos\xi_ivt=0\end{aligned} \tag{64}$$

Equations (61)-(64) can be further epressed as (Zhang *et al*., 2016):

$$\begin{aligned}&\begin{bmatrix}\boldsymbol{M}_{11}&&&\\&\boldsymbol{M}_{22}&&\\&&\boldsymbol{M}_{33}&\\&&&M_{44}\end{bmatrix}\frac{\mathrm{d}^2}{\mathrm{d}t^2}\begin{Bmatrix}\boldsymbol{U}_{1,N\times1}\\\boldsymbol{U}_{2,N\times1}\\\boldsymbol{U}_{3,N\times1}\\Z\end{Bmatrix}+\\&\begin{bmatrix}\boldsymbol{C}_{11}&-\boldsymbol{C}_{12}&\boldsymbol{0}&-\boldsymbol{C}_{14}\\-\boldsymbol{C}_{21}&\boldsymbol{C}_{22}&-\boldsymbol{C}_{23}&\boldsymbol{0}\\\boldsymbol{0}&-\boldsymbol{C}_{32}&\boldsymbol{C}_{33}&\boldsymbol{0}\\-\boldsymbol{C}_{41}&\boldsymbol{0}&\boldsymbol{0}&C_{44}\end{bmatrix}\frac{\mathrm{d}}{\mathrm{d}t}\begin{Bmatrix}\boldsymbol{U}_{1,N\times1}\\\boldsymbol{U}_{2,N\times1}\\\boldsymbol{U}_{3,N\times1}\\Z\end{Bmatrix}+\\&\begin{bmatrix}\boldsymbol{K}_{11}&-\boldsymbol{K}_{12}&\boldsymbol{0}&-\boldsymbol{K}_{14}\\-\boldsymbol{K}_{21}&\boldsymbol{K}_{22}&-\boldsymbol{K}_{23}&\boldsymbol{0}\\\boldsymbol{0}&-\boldsymbol{K}_{32}&\boldsymbol{K}_{33}&\boldsymbol{0}\\-\boldsymbol{K}_{41}&\boldsymbol{0}&\boldsymbol{0}&K_{44}\end{bmatrix}\begin{Bmatrix}\boldsymbol{U}_{1,N\times1}\\\boldsymbol{U}_{2,N\times1}\\\boldsymbol{U}_{3,N\times1}\\Z\end{Bmatrix}=\begin{Bmatrix}\boldsymbol{F}_1\\\boldsymbol{0}\\\boldsymbol{0}\\0\end{Bmatrix}\end{aligned} \tag{65}$$

where $D_i=\sin\xi_ivt$, $H_k=\sin\xi_kvt$, $G_i=\cos\xi_ivt$, $\boldsymbol{M}_{11}$, $\boldsymbol{M}_{22}$, $\boldsymbol{M}_{33}$, $\boldsymbol{K}_{11}$, $\boldsymbol{K}_{22}$, $\boldsymbol{K}_{33}$, $\boldsymbol{K}_{12}$, $\boldsymbol{K}_{23}$, $\boldsymbol{K}_{21}$, $\boldsymbol{K}_{32}$, $\boldsymbol{C}_{11}$, $\boldsymbol{C}_{22}$, $\boldsymbol{C}_{33}$, $\boldsymbol{C}_{12}$, $\boldsymbol{C}_{23}$, $\boldsymbol{C}_{21}$, $\boldsymbol{C}_{32}$ are all $N\times N$ matrices; $\boldsymbol{K}_{14}$, $\boldsymbol{C}_{14}$, $\boldsymbol{F}_1$ are $N\times1$ matrices; and $\boldsymbol{K}_{41}$, $\boldsymbol{C}_{41}$ are $1\times N$ matrices.

$$\boldsymbol{M}_{11}=\begin{bmatrix}m_1+\frac{2M_1}{L}D_1H_1&\frac{2M_1}{L}D_1H_2&\cdots&\frac{2M_1}{L}D_1H_N\\\frac{2M_1}{L}D_2H_1&m_1+\frac{2M_1}{L}D_2H_2&\cdots&\frac{2M_1}{L}D_2H_N\\\vdots&\vdots&\ddots&\vdots\\\frac{2M_1}{L}D_NH_1&\frac{2M_1}{L}D_NH_2&\cdots&m_1+\frac{2M_1}{L}D_NH_N\end{bmatrix}$$

$$\boldsymbol{C}_{23}=\boldsymbol{C}_{32}=\boldsymbol{C}_{33}=\begin{pmatrix}c_2&0&\cdots&0\\0&c_2&\cdots&0\\\vdots&\vdots&\vdots&\vdots\\0&0&\cdots&c_2\end{pmatrix},\ C_{44}=\frac{L}{2}c_0,$$

$$\boldsymbol{K}_{23}=\boldsymbol{K}_{32}=\begin{pmatrix}k_2&0&\cdots&0\\0&k_2&\cdots&0\\\vdots&\vdots&\ddots&\vdots\\0&0&\cdots&k_2\end{pmatrix},\ K_{44}=\frac{L}{2}k_0,$$

$$\boldsymbol{K}_{41}=\begin{bmatrix}k_0D_1\\k_0D_2\\\vdots\\k_0D_N\end{bmatrix}^{\mathrm{T}},\ \boldsymbol{K}_{14}=\begin{bmatrix}k_0H_1\\k_0H_2\\\vdots\\k_0H_N\end{bmatrix},\ \boldsymbol{C}_{14}=\begin{bmatrix}c_0H_1\\c_0H_2\\\vdots\\c_0H_N\end{bmatrix},$$

$$M_{44}=\frac{L}{2}M_2,$$

$$\boldsymbol{K}_{41}=\begin{bmatrix}k_0D_1+c_0v\xi_1G_1 & k_0D_2+c_0v\xi_2G_2 & \cdots & k_0D_i+c_0v\xi_NG_N\end{bmatrix},$$

$$\boldsymbol{C}_{41}=\begin{bmatrix}c_0D_1 & c_0D_2 & \cdots & c_0D_N\end{bmatrix},$$

$$\boldsymbol{K}_{33}=\begin{pmatrix}k_2+\xi_1{}^4E_3I_3 & 0 & \cdots & 0\\ 0 & k_2+\xi_2{}^4E_3I_3 & \cdots & 0\\ \vdots & \vdots & \ddots & \vdots\\ 0 & 0 & \cdots & k_2+\xi_N{}^4E_3I_3\end{pmatrix},$$

$$\boldsymbol{F}_1=\begin{pmatrix}\left(M_1+M_2\right)gH_1\\ \left(M_1+M_2\right)gH_2\\ \vdots\\ \left(M_1+M_2\right)gH_N\end{pmatrix},\ \boldsymbol{M}_{33}=\begin{bmatrix}m_3 & 0 & \cdots & 0\\ 0 & m_3 & \cdots & 0\\ \vdots & \vdots & \ddots & \vdots\\ 0 & 0 & \cdots & m_3\end{bmatrix},$$

$$\boldsymbol{K}_{12}=\boldsymbol{K}_{21}=\begin{pmatrix}k_1 & 0 & \cdots & 0\\ 0 & k_1 & \cdots & 0\\ \vdots & \vdots & \ddots & \vdots\\ 0 & 0 & \cdots & k_1\end{pmatrix},$$

$$\boldsymbol{C}_{12}=\boldsymbol{C}_{21}=\begin{pmatrix}c_1 & 0 & \cdots & 0\\ 0 & c_1 & \cdots & 0\\ \vdots & \vdots & \vdots & \vdots\\ 0 & 0 & \cdots & c_1\end{pmatrix},$$

$$\boldsymbol{M}_{22}=\begin{bmatrix}m_2 & 0 & \cdots & 0\\ 0 & m_2 & \cdots & 0\\ \vdots & \vdots & \ddots & \vdots\\ 0 & 0 & \cdots & m_2\end{bmatrix},$$

$$\boldsymbol{C}_{22}=\begin{pmatrix}c_1+c_2 & 0 & \cdots & 0\\ 0 & c_1+c_2 & \cdots & 0\\ \vdots & \vdots & \vdots & \vdots\\ 0 & 0 & \cdots & c_1+c_2\end{pmatrix},$$

$$\boldsymbol{K}_{22}=\begin{pmatrix}k_1+k_2+\xi_1{}^4E_2I_2 & 0 & \cdots & 0\\ 0 & k_1+k_2+\xi_2{}^4E_2I_2 & \cdots & 0\\ \vdots & \vdots & \ddots & \vdots\\ 0 & 0 & \cdots & k_1+k_2+\xi_N{}^4E_2I_2\end{pmatrix},$$

$$\boldsymbol{C}_{11}=\begin{bmatrix}c_1+\frac{4M_1}{L}v\xi_1G_1H_1+\frac{2c_0}{L}D_1H_1 & \frac{4M_1}{L}v\xi_1G_1H_2+\frac{2c_0}{L}D_1H_2 & \cdots & \frac{4M_1}{L}v\xi_1G_1H_N+\frac{2c_0}{L}D_1H_N\\ \frac{4M_1}{L}v\xi_2G_2H_1+\frac{2c_0}{L}D_2H_1 & c_1+\frac{4M_1}{L}v\xi_2G_2H_2+\frac{2c_0}{L}D_2H_2 & \cdots & \frac{4M_1}{L}v\xi_2G_2H_N+\frac{2c_0}{L}D_2H_N\\ \vdots & \vdots & \vdots & \vdots\\ \frac{4M_1}{L}v\xi_NG_NH_1+\frac{2c_0}{L}D_NH_1 & \frac{4M_1}{L}v\xi_NG_NH_2+\frac{2c_0}{L}D_NH_2 & \cdots & c_1+\frac{4M_1}{L}v\xi_NG_NH_N+\frac{2c_0}{L}D_NH_N\end{bmatrix}$$

$$\boldsymbol{K}_{11}=\begin{bmatrix}E_1I_1\xi_1^4+k_1-\frac{2M_1}{L}\left(v\xi_1\right)^2D_1H_1 & -\frac{2M_1}{L}\left(v\xi_1\right)^2D_1H_2 & \cdots & -\frac{2M_1}{L}\left(v\xi_1\right)^2D_1H_N\\ +\frac{2k_0}{L}D_1H_1+\frac{2c_0}{L}v\xi_1G_1H_1 & +\frac{2k_0}{L}D_1H_2+\frac{2c_0}{L}v\xi_1G_1H_2 & & +\frac{2k_0}{L}D_1H_N+\frac{2c_0}{L}v\xi_1G_1H_N\\ -\frac{2M_1}{L}\left(v\xi_2\right)^2D_2H_1 & E_1I_1\xi_2^4+k_1-\frac{2M_1}{L}\left(v\xi_2\right)^2D_2H_2 & \cdots & -\frac{2M_1}{L}\left(v\xi_2\right)^2D_2H_N\\ +\frac{2k_0}{L}D_2H_1+\frac{2c_0}{L}v\xi_2G_2H_1 & +\frac{2k_0}{L}D_2H_2+\frac{2c_0}{L}v\xi_2G_2H_2 & & +\frac{2k_0}{L}D_2H_N+\frac{2c_0}{L}v\xi_2G_2H_N\\ \vdots & \vdots & \vdots & \vdots\\ -\frac{2M_1}{L}\left(v\xi_N\right)^2D_NH_1 & -\frac{2M_1}{L}\left(v\xi_N\right)^2D_NH_2 & & E_1I_1\xi_N^4-\frac{2M_1}{L}\left(v\xi_N\right)^2D_NH_N\\ +\frac{2k_0}{L}D_NH_1+\frac{2c_0}{L}v\xi_NG_NH_1 & +\frac{2k_0}{L}D_NH_2+\frac{2c_0}{L}v\xi_NG_NH_2 & \cdots & +\frac{2k_0}{L}D_NH_N+k_1\\ & & & +\frac{2c_0}{L}v\xi_NG_NH_N\end{bmatrix}$$

Further, according to the Eqs. (61)-(64), the ordinary differential equations of can be expressed as

$$\boldsymbol{M}\frac{\mathrm{d}^2}{\mathrm{d}t^2}\boldsymbol{U}+\boldsymbol{C}\frac{\mathrm{d}}{\mathrm{d}t}\boldsymbol{U}+\boldsymbol{K}\boldsymbol{U}=\boldsymbol{P}\left(t\right) \tag{66}$$

2.2.3 Solving the equation

Using Eqs. (4)-(6), the following can be obtained

$$U_{n,k}(0)=\int_0^L y_n\left(x,0\right)\sin\left(\xi_kx\right)\mathrm{d}x,\ \ n=1,2,3 \tag{67}$$

$$\frac{\mathrm{d}}{\mathrm{d}t}U_{n,k}(0)=\int_0^L\frac{\mathrm{d}}{\mathrm{d}t}y_n\left(x,0\right)\sin\left(\xi_kx\right)\mathrm{d}x \tag{68}$$

$$\frac{\mathrm{d}^2}{\mathrm{d}t^2}U_{n,k}(0)=\int_0^L\frac{\mathrm{d}^2}{\mathrm{d}t^2}y_n\left(x,0\right)\sin\left(\xi_kx\right)\mathrm{d}x \tag{69}$$

When the SSTBS have zero initial conditions (Ni and Zhang, 2018; Zhang *et al*., 2014):

$$U_{n,k}(0)=0 \tag{70}$$

$$\frac{\mathrm{d}}{\mathrm{d}t}U_{n,k}(0)=0 \tag{71}$$

$$\frac{\mathrm{d}^2}{\mathrm{d}t^2}U_{n,k}(0)=0 \tag{72}$$

Equation (66) is solved by using the initial conditions and substituting the expression of $\boldsymbol{U}$ into Eqs. (7)-(9), the dynamic response of the SSTBS can be obtained as follows.

$$y_n=\frac{2}{L}\sum_{k=1}^{N}U_{n,k}\left(t\right)\sin\left(\xi_kx\right) \tag{73}$$

3 Verifications

3.1 Verifications of proposed method for calculating dynamic response of SSTBS under a moving load

To validate the proposed method for calculating the ses of SSTBS under ang load, the proposed method was compiled in MATLAB R2016a (MATLAB, 2016), and both the proposed method and ANSYS numerical method calculated the dynamic responses of SSTBS at fous with/without considering damping (i.e., 32 m/s, 76 m/s, 100 m/s, and 200 m/s)(Yan and Ren, 2015). They were compared in terms of the time-history curves of dynamic responses and dynamic response peaks of midspan deflections. The finite lysis was conducted by using ANSYS. The COMBIN14 element was used to model the spring and damping, and the spring damper element had longitudinal capability in 1D, 2D or 3D applications. The longitudinal spring-damper option is a uniaxial tension or compression element. BEAM3 was used to model layer-I, layer-II, and layer-III beam. The BEAM3 was a uniaxial element with tension, compression, and bending capabilities (Jiang *et al*., 2018). The material properties and geometric parameters of SSTBS in the proposed method and ANSYS numerical method are as follows: L = 32 m, $E_1=2.06\times10^{11}$ N/m^2, $I_1=3.217\times10^{-5}$ m^4, $E_2=3.5\times10^{10}$ N/m^2, $I_2=1.7\times10^{-3}$ m^4, $E_3=3.45\times10^{10}$ N/m^2, $I_3=10.42$ m^4, $m_1=60$ kg/m, $m_2=1275$ kg/m, $m_3=36000$ kg/m, $k_1=6\times10^7$ N/m^2, $k_2=9\times10^8$ N/m^2, $c_1=9.625\times10^4$ N·s/m^2, $c_2=9.3\times10^4$ N·s/m^2 (Sun *et al*., 2016; Zhan *et al*., 2014).

Comparisons between the calculation results of the proposed method and the ANSYS numerical method are shown in Tables 1-2 and Fig. 3. In Tables 1-2, L_{Ia}, L_{IIa} and L_{IIIa}, respectively represent the calculation results of ANSYS for the peak dynamic responses of layer-I, layer-II, and layer-III midspan deflections. L_{Im}, L_{IIm} and L_{IIIm}, respectively, represent the calculation results of the proposed method for the peak dynamic responses of layer-I, layer-II, and layer-III midspan deflections. E_{I}, E_{II} and E_{III}, respectively, represent the errors between the calculation results of the proposed method and ANSYS numerical method for the midspan deflections peak dynamic responses of layer-I, layer-II, and layer-III. In Fig. 3, $M\text{-}sd_{\mathrm{I}}$, $M\text{-}sd_{\mathrm{II}}$ $M\text{-}sd_{\mathrm{III}}$ represent midspan deflection of layer-I, layer-II, and layer-III, respectively. $C=0$ and $C\neq0$ represent the calculation

Table 1 Comparison of calculation results for dynamic responses of SSTBS under a moving load (C = 0)

Parameter	Speed (m/s)			
	32	76	100	200
L_{Ia} (mm)	-1.07167	-1.09808	-1.17161	-1.12126
L_{Im} (mm)	-1.06379	-1.08264	-1.16877	-1.13122
L_{IIa} (mm)	-0.20908	-0.23271	-0.29848	-0.28792
L_{IIm} (mm)	-0.20918	-0.23177	-0.29805	-0.27666
L_{IIIa} (mm)	-0.17491	-0.20325	-0.23962	-0.27992
L_{IIIm} (mm)	-0.17519	-0.20286	-0.23889	-0.27822
E_{I} (%)	-1.20173	-1.40952	-0.24192	0.88825
E_{II} (%)	0.04772	-0.39654	-0.14345	-3.91253
E_{III} (%)	0.16350	-0.19109	-0.30721	-0.60662

Table 2 Comparison of calculation results for dynamic responses of SSTBS under a moving load ($C\neq0$)

Parameter	Speed (m/s)			
	32	76	100	200
L_{Ia} (mm)	-1.06340	-1.08350	-1.15141	-1.06700
L_{Im} (mm)	-1.06205	-1.07772	-1.14916	-1.06633
L_{IIa} (mm)	-0.20848	-0.23308	-0.30065	-0.28082
L_{IIm} (mm)	-0.20883	-0.23069	-0.29906	-0.27840
L_{IIIa} (mm)	-0.17487	-0.20318	-0.23962	-0.27990
L_{IIIm} (mm)	-0.17517	-0.20283	-0.23896	-0.27822
E_{I} (%)	-0.12658	-0.53383	-0.19538	-0.06233
E_{II} (%)	0.16962	-1.02621	-0.52836	-0.86160
E_{III} (%)	0.16874	-0.16818	-0.27683	-0.60141

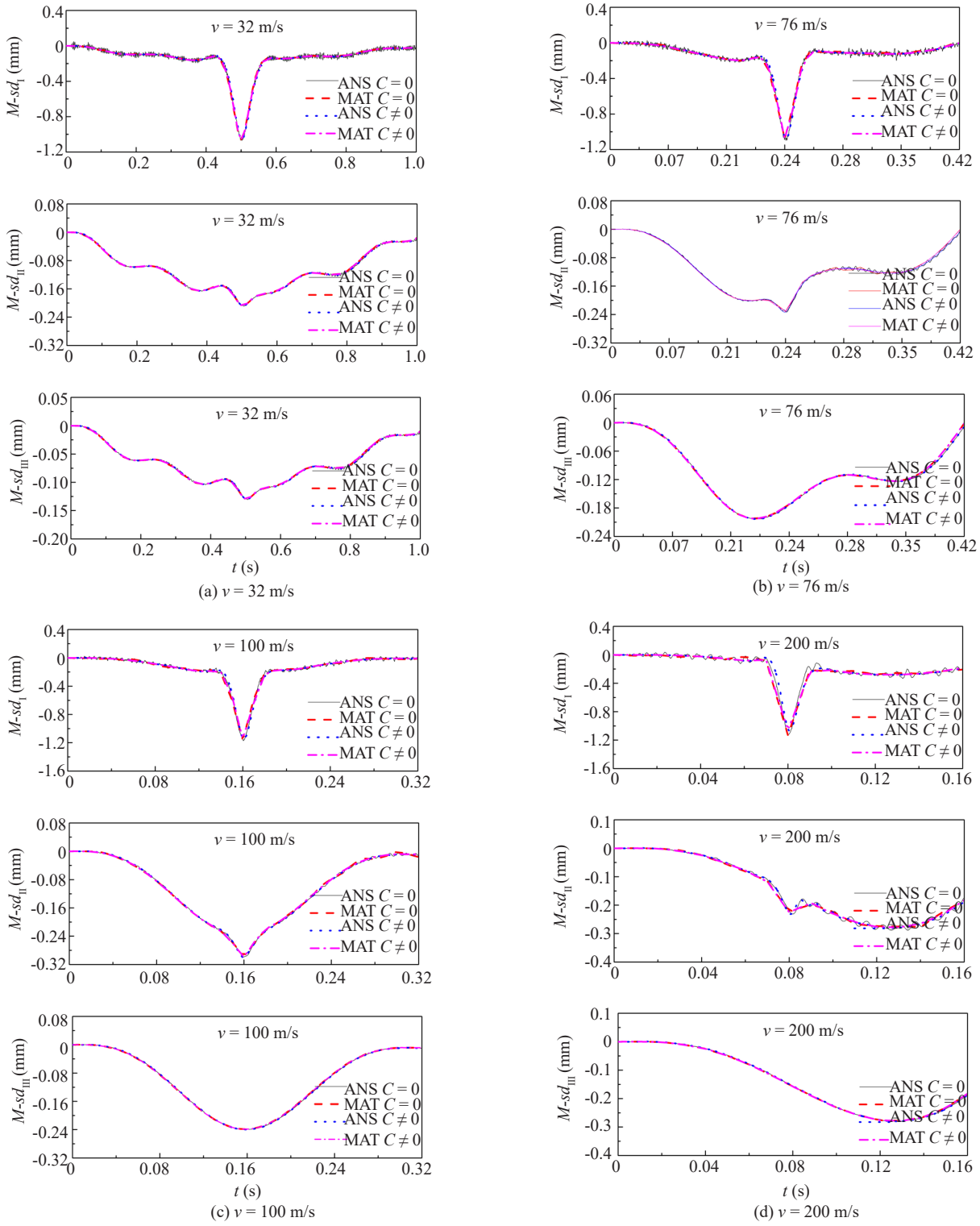

Fig. 3 Calculation result comparison for the time-history curves of the dynamic response of SSTBS at four different speeds under a moving load

without or with considering damping, respectively. ANS and MAT represent the calculation results of the proposed method and ANSYS, respectively.

Tables 1-2 show a comparison of the calculation results for dynamic response peaks of the midspan deflections of layer-I, layer-II, and layer-III in SSTBS at four different speeds under a moving load without or with considering damping. As shown in Tables 1-2, the calculation results of the proposed method for the dynamic response peaks of the midspan deflections of layer-I, layer-II, and layer-III shows good agreement with those of ANSYS; the maximum error is less than 4%, thus validating the analytic method proposed in this study.

Figure 3 shows a comparison of the proposed method and ANSYS numerical calculation results for the dynamic response time–history curves of the midspan deflections of layer-I, layer-II, and layer-III in SSTBS at different speeds under a moving load. As shown in Fig. 3, the proposed method calculation results are consistent with the ANSYS numerical calculation results, further validating the method proposed in this study.

3.2 Verifications of proposed method for calculating dynamic response of SSTBS under a moving mass-spring

To verify the correctness of the proposed method for calculating the dynamic response of SSTBS under a moving mass-spring, and the dynamic responses of SSTBS at four moving speeds (i.e., 32 m/s, 80 m/s, 160 m/s and 200 m/s) were calculated by both the proposed method and ANSYS numerical method. The calculation results were obtained by the two methods for the time-history curves of dynamic responses and the dynamic responses peak of midspan deflections were then compared. The finite element analysis was also conducted by using ANSYS. The element type, geometric parameters and material properties are the same as in Section 3.1. In addition, the MASS21 element, which was a point element having up to six degrees of freedom, was used to model the mass. In addition, k_0 = 3.5×10^6 N/m , c_0 = 2.41×10^3 N·s/m^2, $M_1 = 1000$ kg and $M_2 = 3500$ kg (Lei and Wang, 2014).

Comparisons between the calculation results of the proposed method and ANSYS numerical method are shown in Tables 3-4 and Fig. 4. Tables 3-4 and Fig. 4 provide comparisons of the results for the dynamic responses of midspan deflection peak of layer-I, layer-II, and layer-III under a moving mass-spring at four different speeds. As seen from Tables 3-4, calculation results of the proposed method for the dynamic response peaks of the midspan deflections of these layers are consistent with those from ANSYS; the maximum error is less than 4% without or with considering damping, thus validating the analytic method proposed in this study. According to the Fig. 4, with regard to the dynamic time-history curves of midspan deflections of layer-I, layer-II, and layer-III, the calculation results of the proposed method are in a good agreement with those from the ANSYS numerical method, which further demonstrates the accuracy of the proposed method.

Table 3 Comparison of calculation results for dynamic responses of SSTBS under a moving mass-spring (C = 0)

Parameter	Speeds (m/s)			
	32	80	160	200
L_{Ia} (mm)	-0.5650	-0.6303	-0.9140	-0.8230
L_{Im} (mm)	-0.5569	-0.6505	-0.8945	-0.8007
L_{IIa} (mm)	-0.1053	-0.1230	-0.1550	-0.1550
L_{IIm} (mm)	-0.1064	-0.1232	-0.1541	-0.1531
L_{IIIa} (mm)	-0.1061	-0.1150	-0.1523	-0.1530
L_{IIIm} (mm)	-0.1063	-0.1153	-0.1531	-0.1517
E_{I} (%)	-1.4250	3.2056	-2.1303	-2.7090
E_{II} (%)	1.3257	0.1911	-0.5935	-1.2013
E_{III} (%)	0.1635	0.2635	0.7224	-0.8333

Table 4 Comparison of calculation results for dynamic responses of SSTBS under a moving mass-spring ($C \neq 0$)

Parameter	Speeds (m/s)			
	32	80	160	200
L_{Ia} (mm)	-0.5518	-0.5569	-0.5951	-0.5637
L_{Im} (mm)	-0.5523	-0.5558	-0.5960	-0.5631
L_{IIa} (mm)	-0.1037	-0.1240	-0.1470	-0.1489
L_{IIm} (mm)	-0.1042	-0.1239	-0.1482	-0.1482
L_{IIIa} (mm)	-0.1042	-0.1123	-0.1468	-0.1485
L_{IIIm} (mm)	-0.1045	-0.1126	-0.1479	-0.1479
E_{I} (%)	0.0963	-0.1914	0.1537	-0.1121
E_{II} (%)	0.4768	-0.0746	0.8192	-0.4658
E_{III} (%)	0.2662	0.2293	0.7568	-0.4243

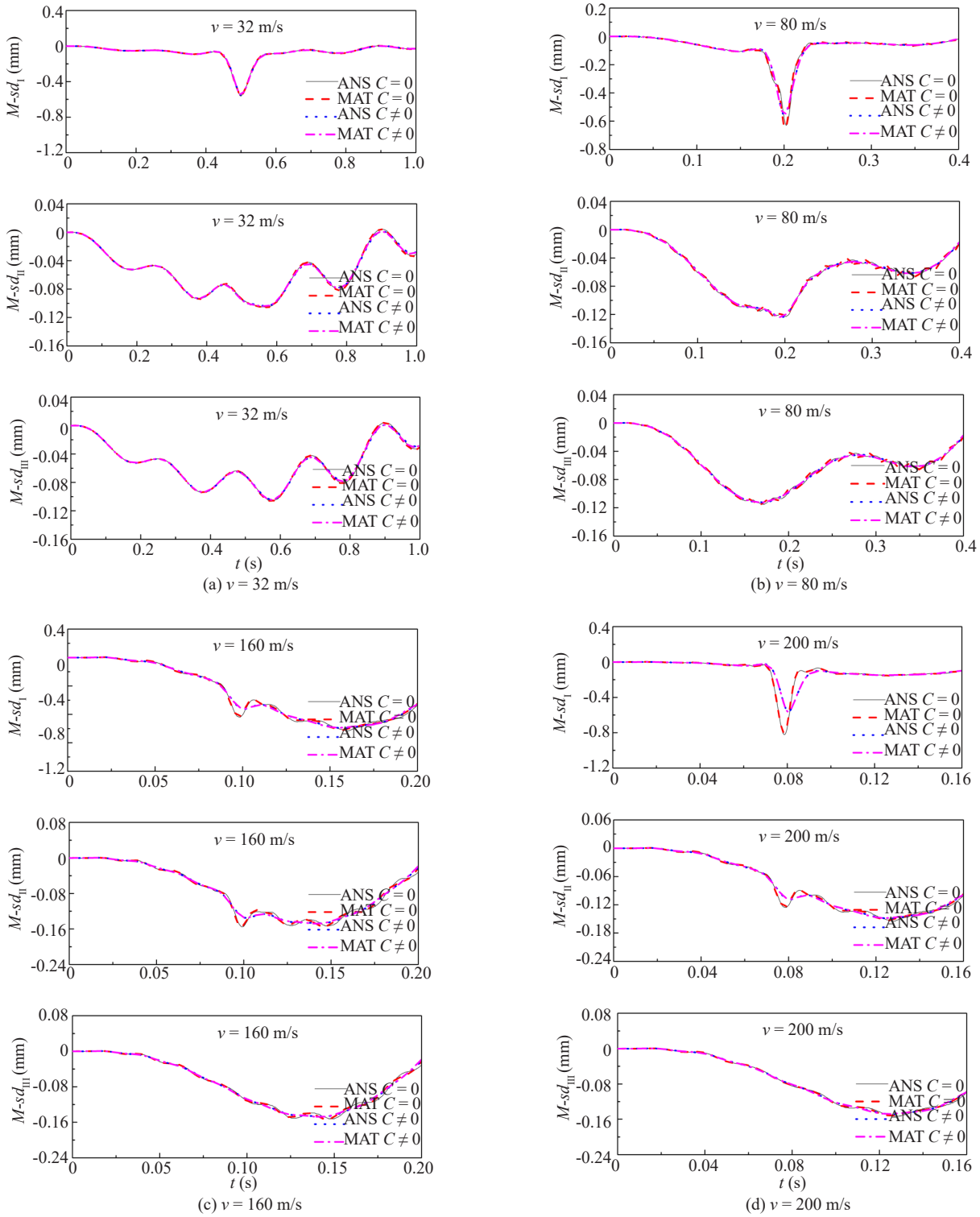

Fig. 4 Calculation result comparison for the time-history curves of the dynamic response of SSTBS at four different speeds under a moving mass-spring

3.3 Damping effect

In order to ascertain the effect of damping on the dynamic responses of SSTBS under a moving load or a moving mass-spring, the effects of damping were obtained from Tables 1-4 and listed in Tables 5-6, where C_{Im}, C_{IIm} and C_{IIIm} represent the effect of damping on the dynamic responses of layer-I, layer-II, and layer-III, respectively.

As seen from Tables 5-6 and Figs. 3-4, the method proposed herein is consistent with the results calculated by the ANSYS numerical method under a moving load

Table 5 Effect of damping on dynamic responses of SSTBS under a moving load

Parameter	Speeds (m/s)			
	32	76	100	200
C_{Im} (%)	0.16	0.46	1.71	6.09
C_{IIm} (%)	0.17	0.47	-0.34	-0.63
C_{IIIm} (%)	0.01	0.01	-0.03	0.00

Table 6 Effect of damping on dynamic responses of SSTBS under a moving mass-spring

Parameter	Speeds (m/s)			
	32	80	160	200
C_{Im} (%)	0.83	17.04	50.08	42.20
C_{IIm} (%)	2.11	-0.55	3.99	3.33
C_{IIIm} (%)	1.73	2.43	3.49	2.56

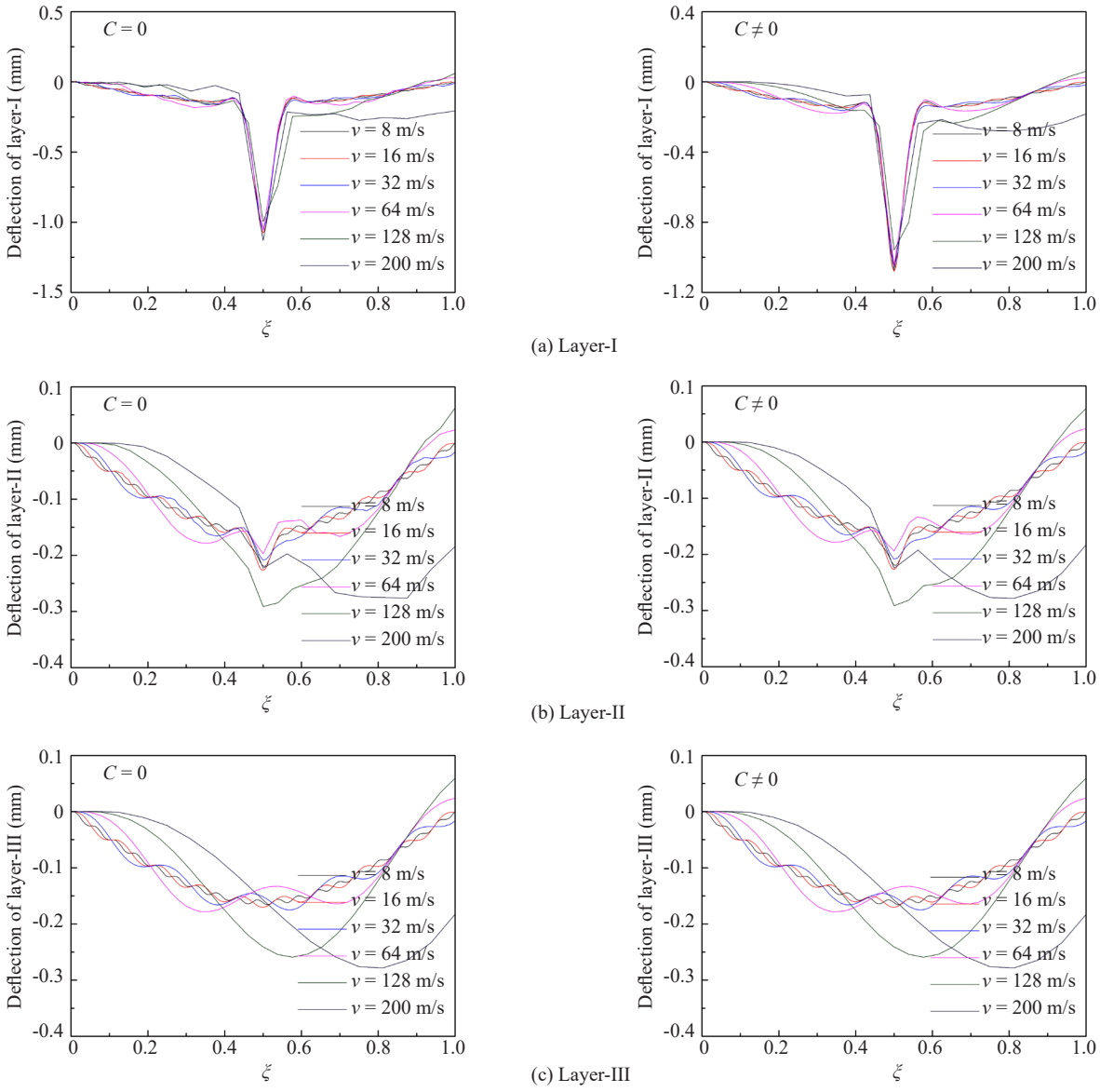

Fig. 5 Deflection responses of SSTBS at different speeds under a moving load

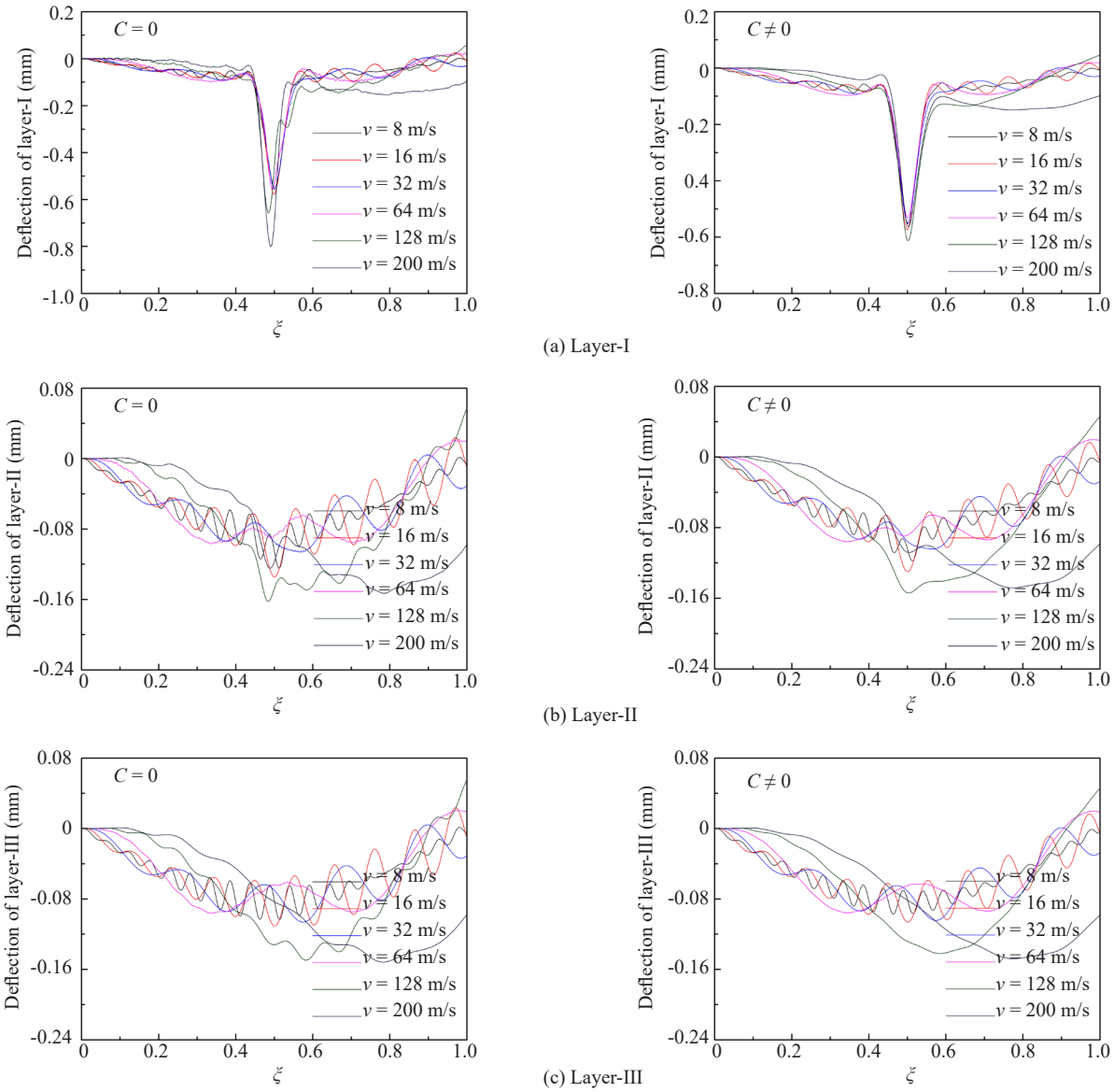

Fig. 6 Deflection responses of SSTBS at different speeds under a moving mass-spring

or a mass-spring considering the effect of damping; the errors are less than -1.03% (under a moving load) and 0.82% (under a moving mass-spring), validating the analytic method proposed in this study. From Tables 3-4 and Figs. 3-4, it can be seen that the damping has the greatest effect on layer-I, then layer-II, and has a smaller effect on layer-III under a moving load or a mass-spring. The effect of damping on three layers of beams all increase as the moving speed increases. Under the moving load, the effect of damping is relatively small, with a maximum of 6%. However, the effect of damping under the moving mass-spring is very large and the maximal value reaches 50%.

4 Applications

Figures 5-6 depict the change of the midspan deflections of three layers without or with considering damping when the load/mass-spring was traveling along the beam at low speeds (8 m/s, 16 m/s), medium speeds (32 m/s, 64 m/s) and high speeds (128 m/s, 200 m/s), where ξ represents the location coordinates of the load/mass-spring on the beam.

As seen from Figs. 5-6, when the moving speed of load/mass-spring increases from 8 m/s to 200 m/s, the peaks of the dynamic responses of SSTBS all increase initially and then subsequently decrease, which shows that for the SSTBS, there is a critical speed. The maximum dynamic deflection always occurs near the midspan of layer-I, and the excitation effect of the load/mass-spring only has a significant effect on the first order frequency. Hence, the investigation of the maximum dynamic deflection of layer-I can be achieved by analyzing the maximum dynamic deflection at the midspan only. However, the shapes of the dynamic deflection curves of layer-II and layer-III vary with the load/mass-spring

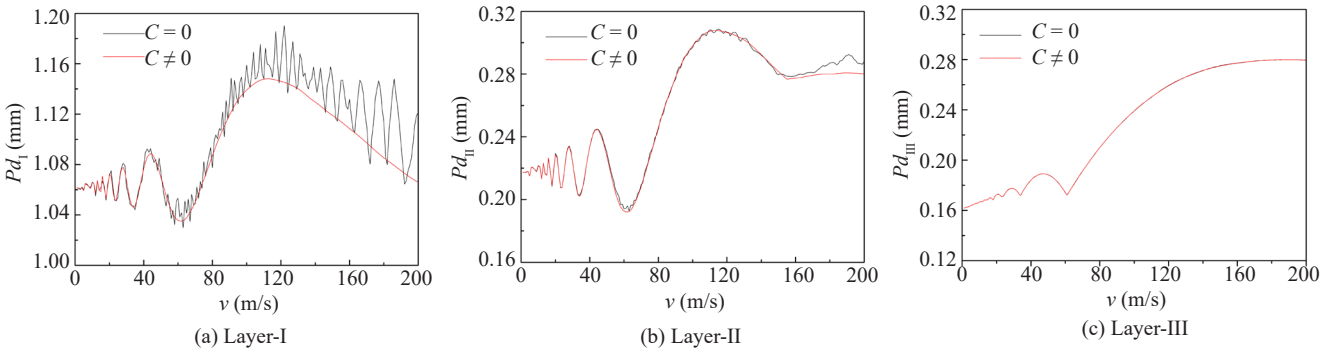

Fig. 7 Relationship curves between the midspan deflections of SSTBS and load moving speeds

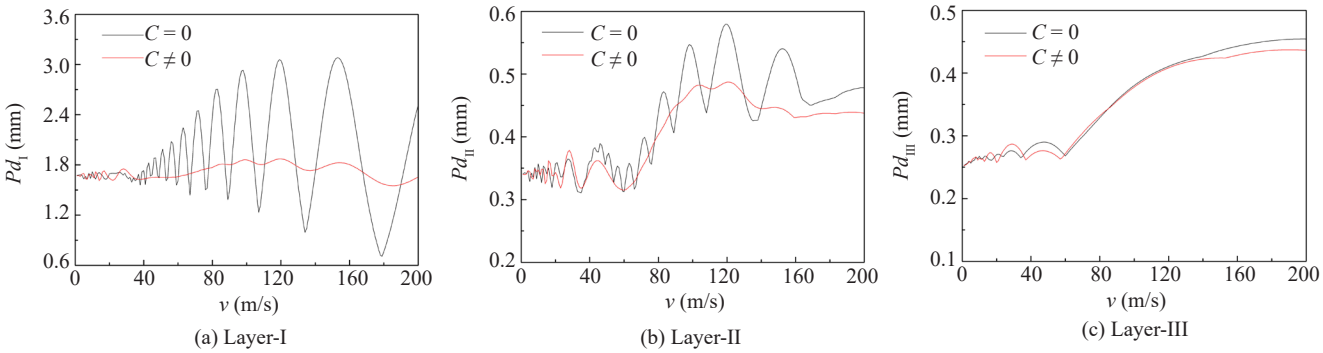

Fig. 8 Relationship curve between the midspan deflection of SSTBS and mass-spring moving speeds

speed, the dynamic response frequency increases as the load/mass-spring speed increases, and the position of the maximum dynamic deflection shifts from the midspan to the traveling direction of the load/mass-spring as the load/mass-spring speed increases.

To study the effect of the load/mass-spring moving speed on the dynamic responses of SSTBS without or with considering damping, the relationship curves between the midspan deflections of layer-I, layer-II, and layer-III and load/mass-spring moving speed were calculated, as shown in Figs. 7-8 where, Pd_{I}, Pd_{II}, Pd_{III} represent peak deflection of layer-I, layer-II, and layer-III, respectively.

As seen from Figs. 7-8, the relationship curves between the midspan deflections of SSTBS and moving speed of the load/mass-spring has several "abrupt increases", suggesting that there is no simple linear relationship between the dynamic responses of the midspan deflections of STTBS and the moving speed of load/mass-spring. This is because when the load/mass-spring travels along a SSTBS, as the speed changes, the loading frequency of the load/mass-spring on the SSTBS changes as well, and when the loading frequency of the load/mass-spring approaches the natural frequency of a certain order of the SSTBS, the structural response reaches its maximum. Thus, the moving speed at which the load/mass-spring causes the SSTBS to experience extreme dynamic responses is not continuous; instead, it occurs at several discontinuous speed points (Zhang *et al.*, 2014). Also, the midspan deflections of SSTBS significantly decreased under a moving load/mass-spring when the effect of damping was considered. The main reason for this is that the addition of damping dissipates a large amount of kinetic energy and reduces the dynamic responses of the SSTBS.

The method proposed herein can be applied to engineering practice. On the right side of Eq. (60) , the first term $\partial^2 y_1 / \partial t^2$ represents the vertical acceleration of SSTBS at the position where the mass was located during vibration; the second term $2v\left(\partial^2 y_1 / \partial x \partial t\right)$

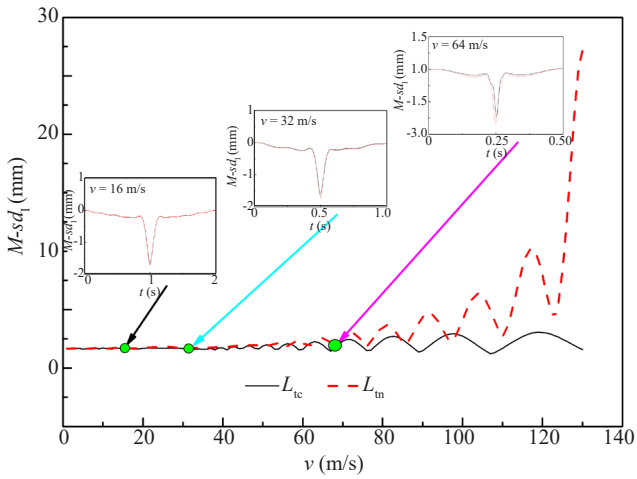

Fig. 9 Midspan deflection and mass-spring moving speed curves of layer-I with or without considering the latter two terms

represents the vertical acceleration incurred by the change in the vertical speed of the SSTBS due to mass movement; and the third term $v^2\left(\partial^2 y_1 / \partial x^2\right)$ represents the centrifugal acceleration produced by mass movement on the vertical curve due to the curvature generated by the SSTBS during vibration (Jia *et al*., 2013). Currently, most studies on dynamic responses neglect the second and third terms, because many believe that considering the terms makes the decoupling of the equations very difficult. For this reason, it is necessary to explore the influence of theso terms on the vibration of the SSTBS. Based on the proposed method, this study investigated the influence of these terms on the dynamic responses of the three layers, as shown in Figs. 9-12. L_{tc} , L_{tn} represent midspan deflection with and without consideringrthe two terms, respectively. L_{tcf} , L_{tcs} represent midspan deflection considering only the first term and only the second term, respectively. In order to clearly reflect the effects of these terms, M_1 and M_2 are modified into 2000 kg and 11500 kg , and the other material properties and geometric parameters are the same as Section 3.2.

As seen from Figs. 9-12, when the moving speed

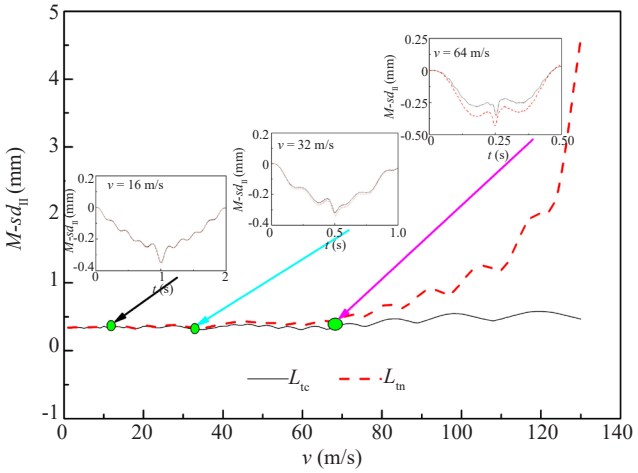

Fig. 10 Midspan deflection and mass-spring moving speed curves of layer-II with or without considering the latter two terms

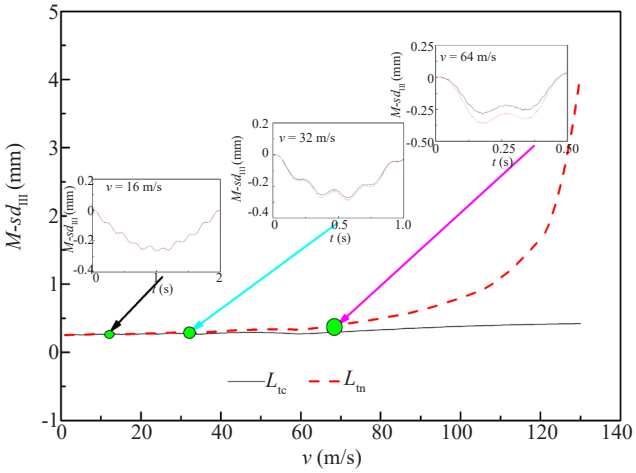

Fig. 11 Midspan deflection and mass-spring moving speed curves of layer-III with or without considering the latter two terms

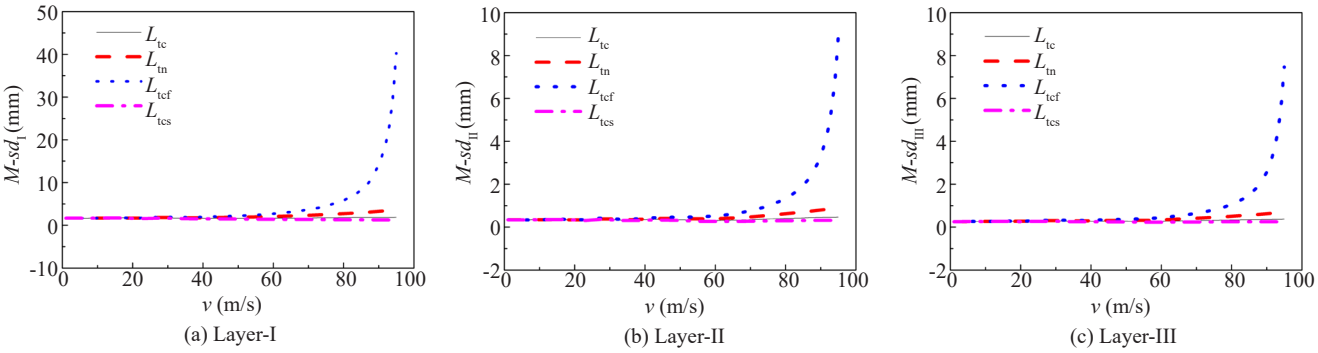

Fig. 12 Midspan deflection and mass-spring moving speed curves of SSTBS considering influences of one of the latter two terms

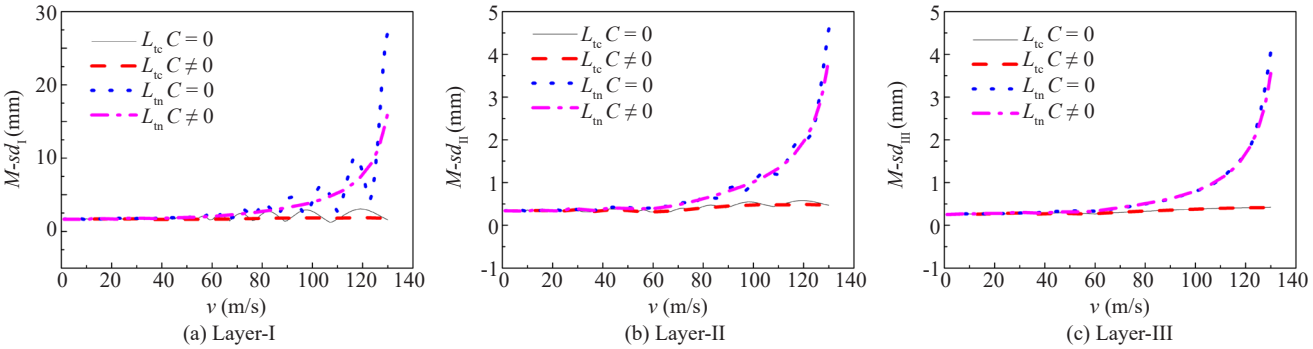

Fig. 13 Midspan deflection and mass-spring moving speed curves of SSTBS with or without considering the latter two terms

of the mass-spring is medium or low, the calculation errors of the midspan deflection of the SSTBS met the requirement for engineering precision whether or not the latter two terms were considered. The calculation errors are generally negligible whenr two terms are not employed at low and medium speeds. However, as the moving speed increases, both the midspan deflection amplitude and vibration frequency became higher. Without considering one of the two terms, the midspan deflection calculation errors of the SSTBS were obviously on the rise. When the speed exceeded 120 m/s, the increase of the calculation error was almost linear, which clearly show thae both terms need to be included in the calculations.

As seen from Fig. 13, the midspan deflections of the SSTBS become significantly small under a moving load/mass-spring after considering the effect of damping, because the structural damping dissipated a large amount of kinetic energy of the SSTBS and reduces the dynamic responses of the SSTBS.

5 Conclusions

(1) Based on finitn Sine-Fourier inverse transform, this study constructed an expression of the dynamic response of the SSTBS under a moving load and a moving mass-spring, respectively, and calculated the dynamic responses of the SSTBS at different speeds. The calculation results obtained in this study show good agreement with the calculation results of the ANSYS numerical method, so the accuracy of the calculation method proposed in this paper was demonstrated. Moreover, due to its clearly defined concept and convenient manual calculation, the calculation method proposed in this study provide a theoretical foundation for further engineering applications of SSTBS under a moving load/mass-spring.

(2) The SSTBS has several critical speeds under the moving load/mass-spring, and the dynamic deflection of layer-I in the SSTBS reaches a maximum value near the midspan at each critical speed.

(3) When the moving speed of the mass-spring was relatively high, neither the vertical acceleration incurred by a change in the vertical speed of the SSTBS due to the movement of the mass-spring nor the centrifugal acceleration produced by the movement of the mass-spring on the vertical curve generated by the SSTBS vibration could be neglected.

(4) The effect of damping on the SSTBS under the moving load is relatively small, and can be neglected in engineering practice. However, the effect of damping under the moving mass-spring is very large and cannot be neglected in engineering practice, especially its effect on layer-I.

Acknowledgement

The research describedrherein was financially supported by the Fundamental Research Funds for the Central Universities of Central South University No. 2018zzts189, the National Natural Science Foundations of China (Nos. 51408449, 51778630), and the Innovation-driven Plan in Central South University under Grant No. 2015CX006.

References

Abu-Hilal M (2006),"Dynamic Response of a Double Euler-Bernoulli Beam Due to a Moving Constant Load," *Journal of Sound and Vibration*, **297**(3): 477–491.

Abu-Hilal M (2007), "Free Transverse Vibrations of a Triple-Beam System," *Journal of Sound and Vibration*, **241**(4): 635–642.

Ba Zhenning, Kang Zeqing and Liang Jianwen (2018), "In-plane Dynamic Green's Functions for Inclined and Uniformly Distributed Loads in a Multi-Layered Transversely Isotropic Half-Space," *Earthquake Engineering and Engineering Vibration*, **17**(2): 293–309.

Bendine K, Boukhoulda FB, Nouari M and Satla Z (2016), "Active Vibration Control of Functionally Graded Beams with Piezoelectric Layers Based on Higher Order Shear Deformation Theory," *Earthquake Engineering and Engineering Vibration*, **15**(4): 611–620.

Dimitrovová Z (2017), "New Semi-Analytical Solution for a Uniformly Moving Mass on a Beam on a Two-Parameter Visco-Elastic Foundation," *International Journal of Mechanical Sciences*, **127**: 142–162.

Jia HY, Zhang DY, Zheng SX, Xie WC and Pandey MD (2013), "Local Site Effects on a High-Pier Railway Bridge under Tridirectional Spatial Excitations: Nonstationary Stochastic Analysis," *Soil Dynamics and Earthquake Engineering*, **52**(6): 55–69.

Jiang LZ, Feng YL, Zhou WB and He BB (2018), "Analysis on Natural Vibration Characteristics of Steel-concrete Composite Truss Beam," *Steel and Composite Structures*, **26**(1): 79–87.

Kumar CPS, Sujatha C and Shankar K (2015), "Vibration of Simply Supported Beams Under a Single Moving Load: A Detailed Study of Cancellation Phenomenon," *International Journal of Mechanical Sciences*, **99**: 40–47.

Lei X and Wang J (2014), "Dynamic Analysis of the Train and Slab Track Coupling System with Finite Elements in a Moving Frame of Reference," *Journal of Vibration and Control*, **20**(9): 1301–1317.

Li C, Li T, Ban D and Ge X (2018), "Equivalent Damping of SDOF Structure with Maxwell Damper," *Earthquake Engineering and Engineering Vibration*, **17**(3): 627–639.

Li J, Chen Y and Hua H (2008), "Exact Dynamic Stiffness Matrix of a Timoshenko Three-Beam System," *International Journal of Mechanical Sciences*, **50**(6): 1023–1034.

Li J and Hua H (2008), "Dynamic Stiffness Vibration Analysis of an Elastically Connected Three-Beam System," *Applied Acoustics*, **69**(7): 591–600.

Li YX, Hu ZJ and Sun LZ (2016), "Dynamical Behavior of a Double-Beam System Interconnected by a Viscoelastic Layer," *International Journal of Mechanical Sciences*, **105**: 291–303.

Li YX and Sun LZ (2016), "Transverse Vibration of an Undamped Elastically Connected Double-Beam System with Arbitrary Boundary Conditions," *Journal of Engineering Mechanics*, **142**(2): 04015070.

Li YX and Sun LZ (2017), "Active Vibration Control of Elastically Connected Double-Beam Systems," *Journal of Engineering Mechanics*, **143**(9): 04017112.

Liu B, Wang YZ and Peng H (2015), "Impact Coefficient and Reliability of Mid-Span Continuous Beam Bridge Under Action of Extra Heavy Vehicle with Low Speed," *Journal of Central South University*, **22**(4): 1510–1520.

Luo N, Jia H and Liao H (2017), "Coupled Wind-Induced Responses and Equivalent Static Wind Loads on Long-Span Roof Structures with the Consistent Load-Response-Correlation Method," *Advances in Structural Engineering*, (3): 136943321770678.

Mao Q (2011), "Free Vibration Analysis of Multiple-Stepped Beams by Using Adomian Decomposition Method," *Mathematical and Computer Modelling*, **54**(1-2): 756–764.

Mao Q and Wattanasakulpong N (2015), "Vibration and Stability of a Double-Beam System Interconnected by an Elastic Foundation under Conservative and Nonconservative Axial Forces," *International Journal of Mechanical Sciences*, **93**: 1–7.

Mathworks (2016), *Matlab Version R2016a*.

Muscolino G and Palmeri A (2007), "Response of Beams Resting on Visco-elastically Damped Foundation to Moving Oscillators," *International Journal of Solids and Structures*, **44**: 1317–1336.

Ni YC and Zhang FL (2018), "Fast Bayesian Approach for Modal Identification Using Forced Vibration Data Considering the Ambient Effect," *Mechanical Systems and Signal Processing*, **105**: 113–128.

Oniszczuk Z (2003), "Forced Transverse Vibrations of an Elastically Connected Complex Simply Supported Double-Beam System," *Journal of Sound and Vibration*, **264**(2): 273–286.

Peng LP, Ai-Min JI, Zhao YM and Liu CS (2017), "Natural Frequencies Analysis of a Composite Beam Consisting of Euler-Bernoulli and Timoshenko Beam Segments Alternately," *Journal of Central South University*, **24**(3): 625–636.

Rezaiee-Pajand M and Hozhabrossadati SM (2014), "Free Vibration Analysis of a Double-Beam System Joined by a Mass-Spring Device," *Journal of Vibration and Control*, **22**(13).

Rusin J, Śniady P and Śniady P (2011), "Vibrations of Double-String Complex System Under Moving Forces. Closed Solutions," *Journal of Sound and vibration*, **330**(3): 404–415.

Shamalta M and Metrikine AV (2003), "Analytical Study of the Dynamic Response of an Embedded Railway Track to a Moving Load," *Archive of Applied Mechanics*, **73**(1-2): 131–146.

Şimşek M (2010), "Vibration Analysis of a Functionally Graded Beam Under a Moving Mass by Using Different Beam Theories," *Composite Structures*, **92**(4): 904–917.

Şimşek M (2011), "Nonlocal Effects in the Forced Vibration of an Elastically Connected Double-Carbon Nanotube System under a Moving Nanoparticle," *Computational Materials Science*, **50**(7): 2112–2123.

Şimşek M (2015), "Bi-Directional Functionally Graded Materials (Bdfgms) for Free and Forced Vibration of Timoshenko Beams with Various Boundary Conditions," *Composite Structures*, **133**: 968–978.

Şimşek M and Cansız S (2012), "Dynamics of Elastically Connected Double-Functionally Graded Beam Systems with Different Boundary Conditions under Action of a Moving Harmonic Load," *Composite Structures*, **94**(9): 2861–2878.

Sun LM, Xie WP, He XW and Hayashikawa T (2016), "Prediction and Mitigation Analysis of Ground Vibration Caused by Running High-Speed Trains on Rigid-Frame Viaducts," *Earthquake Engineering and Engineering Vibration*, **15**(1): 31–47.

Sun L, Hayashikawa T, He X and Xie W (2015), "Influential Parameter Analysis on Vibration Responses of Rigid-Frame Viaducts Induced by Running High-Speed Trains," *International Journal of Steel Structures*, **15**(4): 809–826.

Sun L, He X, Hayashikawa T and Xie W (2015), "Characteristic Analysis on Train-Induced Vibration Responses of Rigid-Frame Rc Viaducts," *Structural Engineering and Mechanics*, **55**(5): 1015–1035.

Wang Z and Ren W (2013), "Crack Detection Using Integrated Signals from Dynamic Responses of Girder Bridges," *Journal of Central South University*, **20**(6): 1759–1766.

Wu Y and Gao Y (2015), "Analytical Solutions for Simply Supported Viscously Damped Double-Beam System under Moving Harmonic Loads," *Journal of Engineering Mechanics*, **141**(7): 04015004.

Wu Y and Gao Y (2016), "Dynamic Response of a Simply Supported Viscously Damped Double-Beam System under the Moving Oscillator," *Journal of Sound and Vibration*, **384**: 194–209.

Yan WJ and Ren WX (2013), "Use of Continuous-Wavelet Transmissibility for Structural Operational Modal Analysis," *Journal of Structural Engineering*, **139**(9): 1444–1456.

Yan WJ and Ren WX (2015), "An Enhanced Power Spectral Density Transmissibility Approach

for Operational Modal Analysis: Theoretical and Experimental Investigation," *Engineering Structures*, **102**: 108–119.

Yang YB and Lin CW (2005), *Vehicle-Bridge Interaction Dynamics and Potential Applications*, Directory of documentation, libraries and archives services in Africa, Unesco.

Zhai WM and Cai CB (2011), *Train-Track-Bridge Dynamic Interaction: Theory and Engineering Application*, Science Press, Beijing.

Zhan Y, Yao H, Lu Z and Yu D (2014), "Dynamic Analysis of Slab Track on Multi-Layered Transversely Isotropic Saturated Soils Subjected to Train Loads," *Earthquake Engineering and Engineering Vibration*, **13**(4): 731–740.

Zhang DY, Jia HY, Zheng SX, Xie WC and Pandey MD (2014), "A Highly Efficient and Accurate Stochastic Seismic Analysis Approach for Structures under Tridirectional Nonstationary Multiple Excitations," *Computers and Structures*, **145**(C): 23–35.

Zhang FL, Ni YC, Au SK and Lam HF (2016), "Fast Bayesian Approach for Modal Identification Using Free Vibration Data, Part I-Most Probable Value," *Mechanical Systems and Signal Processing*, **s70-71**: 209–220.

Zhang YQ, Lu Y and Ma GW (2008), "Effect of Compressive Axial Load on Forced Transverse Vibrations of a Double-Beam System," *International Journal of Mechanical Sciences*, **50**(2): 299–305.

Zheng DY (2000), "Vibration of Vehicle on Compressed Rail on Viscoelastic Foundation," *Journal of Engineering Mechanics*, **126**(11): 1141–1147.